UNIVERSITÀ DEGLI STUDI DI PARMA

Department of Life sciences

Ph.D. Program in Biotechnology

XXIX cycle

Transthyretin and Retinol-Binding-Protein system: from functional and structural properties to pathological implications

Coordinator of the Ph.D. program:

Professor Nelson Marmiroli

Tutor:

Professor Rodolfo Berni

Ph.D. Student:

ALBERTO FERRARI

2014-2016

Index:

PART III: Functional analysis of two pathological forms of human Retinol Binding Protein (RBP)

INTRODUCTION

In this Doctorate thesis, functional and structural properties of the two human proteins Transthyretin (TTR) and Retinol-binding Protein (RBP, also known as RBP4), which form in plasma a macromolecular complex, and their relationships with human pathological states have been investigated. TTR is a homotetrameric protein of approximatively 55KD, physiologically involved in the distribution of thyroid hormones (thyroxine and triiodothyronine), together with other binding proteins (Bartalena & Robbins, 1993;Richardson, 2005) and in the co-transport of vitamin A, by forming in plasma the TTR-RBP complex (Monaco, Rizzi, and Coda 1995). TTR was generated during early vertebrate evolution as a result of a duplication event in the gene encoding 5-hydroxyisourate hydrolase, one of the enzyme involved in the degradation pathway of uric acid and present in different prokaryotes and eukaryotic lineages (Hennebry et al. 2006; Jung et al. 2006; Ramazzina et al. 2006; Zanotti et al. 2006; French and Ealick 2011). RBP is a monomeric protein of approximatively 21KDa which mediates the delivery of retinol (alcoholic form of Vitamin A) to the target cells (Cowan, Newcomer, and Jones 1990; Zanotti and Berni 2004), where a membrane receptor STAR6 (Stimulated by retinoic acid) permit retinol uptake (Kawaguchi et al., 2007; Redondo, Vouropoulou, Evans, & Findlay, 2007; Chen et al., 2016). TTR and RBP are synthesized primarily by the hepatocytes and are secreted into the circulation, where RBP is found bound to TTR. This feature is believed to be of physiological significance, reducing the glomerular filtration of the relatively small RBP (Episkopou et al., 1993; van Bennekum et al., 2001) and strengthening the retinol-RBP complex (Goodman & Raz, 1972; Folli, Viglione, Busconi, & Berni, 2005). The stability of the TTR-RBP complex is strongly affected by the presence of retinol bound to RBP, and as a result the affinity of holo-RBP for TTR is significantly higher than that of apo-RBP (Malpeli, Folli, and Berni 1996; Fex, Albertsson, and Hansson 1979). This features is consistent with holo-RBP being retained in the circulation and with the uncomplexed apo-RBP being excreted by glomerular filtration. TTR is one of more than 30 proteins associated with a group of human diseases known as amyloidoses, characterized by the extracellular deposition of aggregates, in the form of fibrils (Sekijima 2015; Ankarcrona et al. 2016). To date, more than 100 point mutations have been described for TTR, most of which are involved in familial amyloidoses (Connors et al. 2003; Benson and Kincaid 2007; Sekijima et al. 2012). Moreover, RBP has also been associated with human diseases, such as night blindness (Biesalski et al. 1999) and congenital eye malformations (MAC disease) (Chou et al. 2015).

1.1 Transthyretin (TTR)

1.1.1 Thyroid hormones (THs) transporter

The thyroid hormones (THs) triiodothyronine (T_3) and its pro-hormone thyroxine (T4) (**Figure 1**) play key physiological roles. During prenatal growth THs are essential for correct tissues development whereas during adult life THs regulate heat generation, carbohydrate and lipid metabolism and function as transcriptional activator for different genes. Both excess and deficiency of THs lead to disorders known as hyperthyroidism and hypothyroidism, respectively.

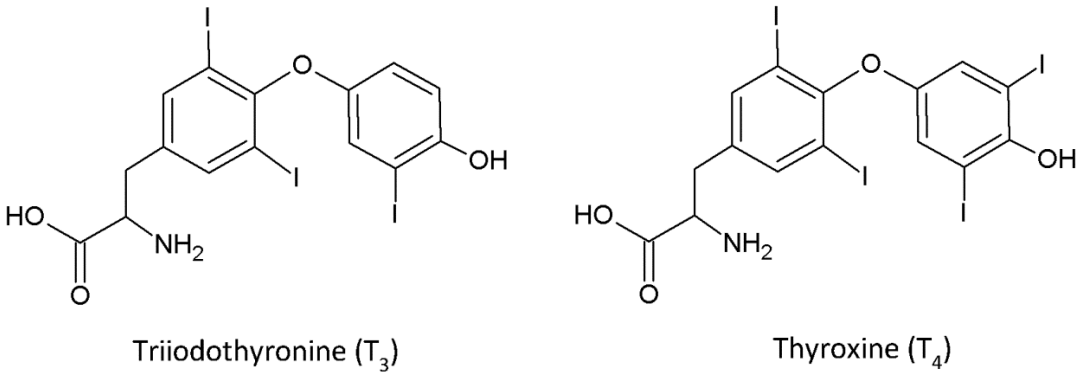

Figure 1.

THs are produced by the thyroid gland an secreted into the blood stream where more than 99% of the THs is bound to three specific plasma proteins that ensure the circulation of THS in the blood, preventing partitioning of THs into lipid membrane of cells (Richardson et al. 2015). Of these, thyroxine binding globulin (TBG) shows the highest affinity, transthyretin (TTR) intermediate affinity and serum albumin (HSA) the lowest affinity. **Table 1** report, for each protein, the concentration, contribution to the hormones binding and the association constants (Bartalena and Robbins 1993).

	Concentration in Human Plasma (mg/ml)	Approximate Contribution to Hormone Binding (%)		Association Constant (M^{-1})	
		T3	T4	T3	T4
TBG	0.15	75	65	$4.6x10^8$	$1x10^{10}$
TTR	2.5	10	10	$1.4x10^7$	$7x10^7$
HSA	420	10	20	$1x10^5$	$7x10^5$

Table 1. Contribution to THs binding and association constant of the three main THs transporter (Bartalena and Robbins 1993)

Transthyretin (TTR, formerly called prealbumin), is principally synthesized in liver, and to a minor extent in choroid plexus and retina . When secreted into the blood stream it works not only as thyroxine (T4) transporter (Wojtczak et al. 1996) but it also binds retinol binding protein (RBP) in order to help the circulation of retinol (Vitamin A) in plasma (Monaco, Rizzi, and Coda 1995). TTR expressed in the choroid plexus becomes the principal transporter of (T4) in cerebrospinal fluid (CSF) (Bartalena and Robbins 1993).

1.1.2 TTR structure

TTR is an oligomeric protein of approximatively 55KDa made up of four identical monomeric units each composed by 127 amino acid residues. **Figure 2** shows the tetrameric and the dimeric forms of TTR. Each monomer is composed of eight anti-parallel β-strands, denoted A-H, organized in two four antiparallel-stranded β-sheets: the inner sheet DAGH and the outer sheet CBEF, that assume a topology similar to the classical Greek key β-barrel. A short α-helix is located between strands E and F. Two monomers dimerise through an intermolecular main-chain interaction involving the H-strands (residues from Ser115 to Thr123) and the F strand (residues Ala91 to Ala97) from each monomer. Monomer inner sheet DAGH forms with its homologous HGAB of the other monomer a pseudo-continuous eight stranded β-sheets (**Figure 3**). While dimers are mainly kept together by hydrogen bonds, two dimers interact through hydrophobic contacts involving residues situated in the AB and GH-loops (Blake et al. 1978; Hörnberg et al. 2000).

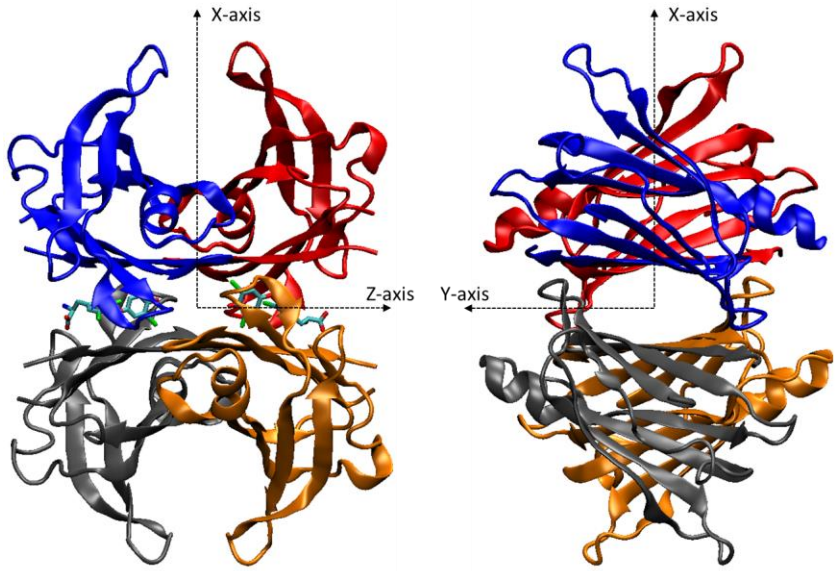

Figure 2. Ribbon diagram depiction of the human wt-TTR-$(T4)_2$ cocrystal structure viewed perpendicular and down the Z-axis (which passes through the T4 binding channel)

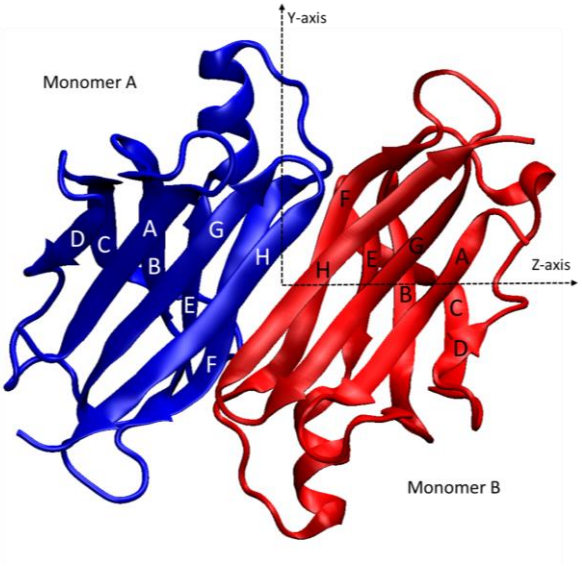

Figure 3. Ribbon diagram of the AB dimer interface

1.1.3 TTR binding sites

One of the 3-fold symmetry axes of TTR (Z-axis) coincides with a long channel that transverses the entire tetramer and harbours two symmetrical binding sites for T4, at the dimer-dimer interface. Structural analysis of the TTR-T4 complex showed that the hormone binding site is characterized by a series of subsites, an outer binding subsite, an inner binding subsite and an intervening interface that are all composed of pairs of symmetric hydrophobic depression referred as halogen binding pockets (HBPs). HBP 1, 1' and HBP 2, 2' are in the outer binding subsite whereas HBP 3 and 3' are localized in the inner binding subsite (**Figure 4**) (Wojtczak et al. 1996) .

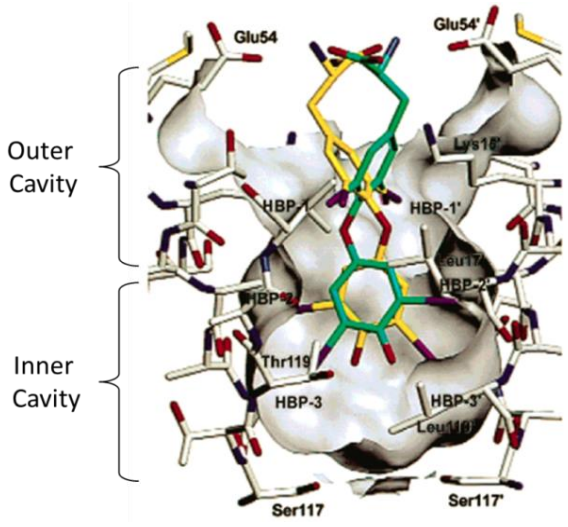

Figure 4. Expanded view of the T4 binding pocket with bound T4 shown in its two symmetry-related binding modes (Green and Yellow) (Klabunde et al. 2000)

TTR binding sites are very similar and both occupied in the crystal (Wojtczak et al. 1996), while the binding of T4 in solution is strongly affected by a negative binding cooperativity. Biochemical studies revealed a 100-fold difference between binding constants for the first and the second binding site (Ferguson et al. 1975). It has been suggested that the lower affinity of T4 for the second binding site may be related to conformational changes due to the binding of T4 in the first site (Muzioł, Cody, and Wojtczak 2001). Haupt et al. (2014) showed that the Ser117 of each monomers (A, A', B and B') that narrow the cavity on the bottom of the cleft, may play a pivotal role in changing binding sites conformation. Joint neutron and X-ray crystallographic analysis show an asymmetry at the dimer-dimer interface, due to a single water molecule complex between Ser117 of monomers A and A' or of monomers B and B'. The interchanging of the water molecule between the two sites leads to a formation of a slightly bigger site that becomes the one with the higher affinity.

TTR binding sites are able to accommodate different small molecules in addition to T4, for example polyphenols, representing a large family of natural compounds, widely distributed in the plant kingdom, which are characterized by the presence of multiple phenolic groups in their molecules. Polyphenols are the most abundant antioxidants present in human diet and resveratrol is one of the best known. Among them different studies provided evidence for the specific interaction of resveratrol (Klabunde et al. 2000, Florio et al. 2015) and of some flavonoids with the T4 binding sites (Radović, Mentrup, and Köhrle 2006, Florio et al. 2015). Moreover recent data have indicated the presence of distinct preferential binding sites in TTR for T4 and some polyphenols (Florio et al. 2015). Cianci et al. (2015) demonstrated by X-ray analysis of three ligand-TTR complexes that the two TTR binding sites can present significantly different occupancy with a preferential ligand binding site in the crystal.

1.1.4 The TTR-RBP complex

Retinol Binding Protein (RBP) and TTR are co-secreted as a complex by hepatocytes and this association increases the stability of the retinol-RBP complex (Goodman and Raz 1972; Folli et al. 2005) and reduces the glomerular filtration of the relatively small RBP molecule (Episkopou et al. 1993, van Bennekum et al. 2001). In turn, the RBP-bound retinol strongly affects the interaction between RBP and TTR, so that the affinity of holo-RBP for TTR is significantly higher than that of apo-RBP, with Kd values of 0.2 µM and 1.2µM respectively (Malpeli, Folli, and Berni 1996). This finding is consistent with holo-RBP being retained in the circulation as protein-protein complex

and with the apo-RBP, resulting from the delivery of retinol, being selectively cleared from the circulation by glomerular filtration. The TTR fully saturated by RBP is characterized by a 1:2 stoichiometry (**Figure 5.a**), to form a complex in which each one RBP molecule interacts simultaneously with three TTR subunits (**Figure 5.b)** (Monaco, Rizzi, and Coda 1995, Naylor and Newcomer 1999, Zanotti et al. 2008). However, it should be noted that the concentration of TTR in plasma is significantly higher than that of RBP, so that *in vivo* a 1:1 TTR-RBP complex can be formed (Episkopou et al. 1993).

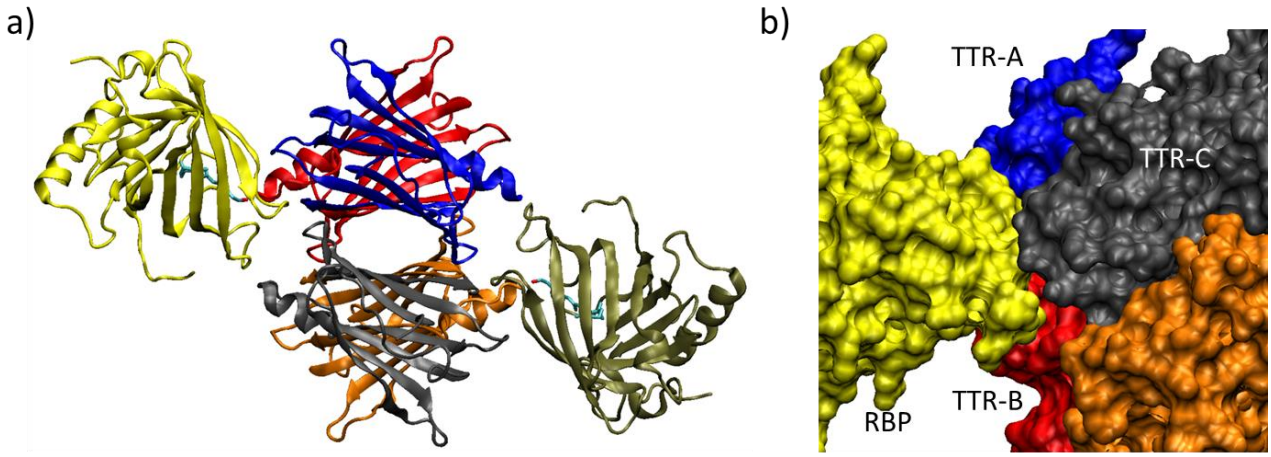

Figure 5. a) Ribbon diagram depiction of the TTR-$(RBP)_2$ complex; **b)** Surface representation of the interaction between RBP and TTR subunits A, B and C (Zanotti et al. 2008)

In the protein-protein complex, RBP and TTR maintain virtually the structure they have in their uncomplexed state, with only minor changes in contact regions. The amino acid residues of RBP that are involved in protein-protein interactions are located in the region of entrance of retinol in the β-barrel cavity (loops 32-36, 63-67 and 92-98). The contact surface of TTR is characterized by a prevalence of hydrophobic residues in the case of monomers B and C and of hydrophilic residues in the case of monomer A. Zanotti et al. (2008) conducted a structural study on TTR mutants in order to assess the relevance of TTR residues in complex formation with RBP. They demonstrated that despite a few exceptions, the substitutions of hydrophilic for hydrophobic side chains in TTR contact regions generally have a rather pronounced dissociation effect on TTR-RBP complex, consistent with the important role played by interfacial apolar interactions. The changes in the TTR molecule induced by amyloidogenic mutations do not interfere with the TTR-RBP complex formation, unless the mutations are located in contact areas, such as Ile84Ser (Zanotti et al. 2008, Berni et al. 1994). Also, retinol participates in the recognition of TTR. In fact, its hydroxyl end

group, which points towards TTR, can take part in a hydrogen bond with the peptide carbonyl group of Gly83 (Monaco, Rizzi, and Coda 1995). Malpeli et al. (1996) demonstrated the importance of the retinol hydroxyl group for the interaction of human TTR with retinoid-RBP complexes. Remarkably, they showed that the complex of RBP with fenretinide, which lacks the hydroxyl end group, exhibits negligible affinity for TTR.

1.2 TTR amyloidoses

According to the official International Society of Amyloidosis (ISA), there are more than 30 human genes associated with amyloidoses (**Table 2**) (Sipe et al. 2014). The misfolding or misassembly of these proteins leads to the formation of a cross-β-sheet structural motif, which is the hallmark of these disorders (Kelly 1996; Dobson 2003). The development of amyloidosis is often linked to ageing, as in the case of Alzheimer's disease and the type 2 diabetes mellitus. The deposition of insoluble aggregates can occur systematically or is localized in specific organs and tissues. Systemic forms of amyloid diseases, often linked to ageing but less common, include the TTR amyloidoses (Ankarcrona et al. 2016). The origin of TTR amyloidoses is either sporadic (caused by the wt protein) or hereditary (familial), due to mutated TTR forms (Benson and Kincaid 2007; Connors et al. 2003; Sekijima et al. 2012).

Amyloidosis type	Precursor protein	Syndrome
Aβ	Amyloid β precursor protein	Alzheimer's disease
		Aging
AApoAI	Apolipoprotein A-I	Familial amyloidosis
		Atherosclerosis
AApoAII	Apolipoprotein A-II	Familial amyloidosis
AApoAIV	Apolipoprotein A-IV	Sporadic amyloidosis associated with aging
AH	Immunoglobulin heavy chain	Sporadic amyloidosis associated with plasma cell dyscrasia
AL	Immunoglobulin light chain	Sporadic amyloidosis associated with plasma cell dyscrasia
AIAPP	Islet amyloid polypeptide (amylin)	Type 2 diabetes
		Insulinoma
		Aging
AMed	Lactadherin/medin	Aortic medial amyloidosis associated with aging
ALys	Lysozyme	Familial amyloidosis
$A\beta_2M$	β_2-Microglobulin	Hemodialysis-associated amyloidosis
APrP	Prion protein	Spongiform encephalopathies
AA	Serum amyloid A	Sporadic reactive amyloidosis
ATTR	Transthyretin	Familial amyloidosis
		Sporadic amyloidosis associated with aging

Table 2. Some amyloidogenic proteins and related amyloidoses are reported (Westermark, Fändrich, and Westermark 2015)

TTR is a normally structured protein which is believed to undergo dissociation into monomers, which in turn may undergo misfolding and misassembly, thereby leading to amyloid fibril

formation (Colon and Kelly 1992, Lai, Colón, and Kelly 1996). TTR amyloidoses can be divided in two main categories: hereditary and acquired diseases.

Acquired amyloidosis: it's a common ageing related phenomenon, involving deposition of wt TTR fibrils in systemic organs in the old age. Typically, patients with acquired amyloidosis show mainly, but not exclusively, cardiac manifestations, such as congestive heart failure, atrial fibrillation and intractable arrhythmia (Sekijima 2015).

Hereditary amyloidoses: these are the most common forms of amyloidosis caused by mutated TTR. These kind of pathologies are life threatening diseases, that may present with peripheral neuropathy, autonomic neuropathy, cardiomyopathy, ophthalmopathy and leptomeningeal amyloidoses. Familial amyloid polyneuropathy (FAP), familial amyloid cardiomyopathy (FAC) and familial leptomeningeal amyloidoses are the three main phenotypes (**Table 3**). Despite the presence of the same mutation in different patients, the phenotype associated with a specific mutation is not always uniform.

- Familial amyloid polyneuropathy (FAP): this is the most common clinical phenotype characterized by a prevalent deposition of amyloid fibrils in peripheral nerves, that lead to autonomic neuropathy, neurogenic bladder, loss of all sensory modalities cardiomyopathy. Val30Met is one of the most common TTR mutation associated with this disease. (Sekijima 2015).
- Familial amyloid cardiomyopathy (FAC): this is another common clinical phenotype characterized by a prevalent amyloid deposition in the cardiovascular system leading to congestive heart failure, intractable arrhytmia and conduction block. Val122Ile is one of the most common transthyretin mutations associated with this disease (Sekijima 2015).
- Familial leptomeningeal amyloidoses: they are characterized by deposition of amyloid fibrils in the leptomeninges and it is restricted to a certain number of mutations, such as Asp18Gly, Ala25Thr and Tyr114Cys. These variants are the most destabilized, with the fastest dissociating TTR tetramers, and because of their instability, these proteins are mostly degraded in the liver by the ER-associated degradation (ERAD), so that they are not secreted in the bloodstream (Sekijima et al. 2005). In these diseases the main source of TTR variant is the choroid plexus, where TTR transports T4, coming from the bloodstream, to the cerebrospinal fluid (CSF). TTR can't cross the blood-CSF barrier, but TTR expressed by the choroid plexus epithelial cells that bind T4 can be secreted in the CSF (Dickson et al.

1987, Schreiber et al. 1990). The high concentration of T4 in choroid plexus acts as a native state stabilizer allowing folding and secretion, but once secreted the tetramer dissociate, resulting in amyloid deposition in the leptomeninges.

These TTR variants cause cerebral infarction, cerebral haemorrhage, hydrocephalus and various central nervous dysfunctions such as ataxia and dementia (Sekijima 2015).

Precursor proteins	Clinical Phenotypes	Representative *TTR* genotypes	Effective disease-modifying therapies	Ongoing clinical trials
Variant TTR	Hereditary ATTR amyloidosis			
	Familial amyloid polyneuropathy (FAP)	Val30Met (p.Val50Met) Leu58His (p.Leu78His)	Liver transplantation Tafamidis Diflunisal	ASOs* (ISIS-TTRRX, Phase III) siRNA** (ALN-TTR02, Phase III) Doxy-TUDCA*** (Phase II)
	Familial amyloid cardiomyopathy (FAC)	Val122Ile (p.Val142Ile) Leu111Met (Leu131Met)	Combined heart and liver transplantation	Tafamidis (Phase III) siRNA** (ALN-TTRsc, Phase II)
	Familial leptomeningeal amyloidosis	Asp18Gly (p.Asp38Gly) Ala25Thr (p. Ala45Thr)	None	None
Wild-type TTR	Wild-type ATTR (ATTRwt) amyloidosis	Wild-type	None	Tafamidis (Phase III) siRNA** (ALN-TTRsc, Phase II)

Table 3. Clinical spectrum of transthyretin amyloidoses (Sekijima 2015)

1.2.1 Process of TTR amyloid fibril formation

A wide range of proteins and peptides with no sequence similarity or common native motifs have been shown to form amyloid fibrils, by self-assembling into insoluble cross-β-sheet quaternary structural forms (Serpell, Sunde, and Blake 1997). The cross β-sheet structure for TTR was shown for the first time by Blake and Serpell (1966) by means of X-ray analysis of *ex vivo* fibrils, in which four β-helical protofilaments adopt a cross-β-sheet structure (corresponding to individual strands oriented perpendicular to the long axis of the fibrils) and associate to form an amyloid fibril (**Figure 6**). The conversion of the native folded TTR tetramer into insoluble amyloid fibrils is a dynamic multistep process and it is widely accepted that TTR tetramer dissociation into monomer is the rate limiting step that allows subsequent aggregation into insoluble fibrils (Colon and Kelly 1992, Lai, Colón, and Kelly 1996). Amyloid formations is generally considered to be a nucleation dependent process (**Figure 7.a**), where fibril growth requires the formation of an oligomeric high-energy quaternary structure before monomers addition can become energetically favourable. As demonstrated by Hurshman et al. (2004), amyloid formation by the TTR monomer proceeds by spontaneous energetically downhill polymerisation, where the rate limiting step is tetramer to monomer transition (**Figure 7.b**). Amyloidogenic variants variably decrease protein thermodynamic stability, favouring the shift towards unfolded monomeric species, promoting tetramer dissociation and monomer unfolding (Hammarström et al. 2002)

Figure 6. Illustration of isolated protofilament (left) and the model of the core structure (right) viewed normal to the filament axis (top) and along the filament axis (bottom) (Blake and Serpell 1996).

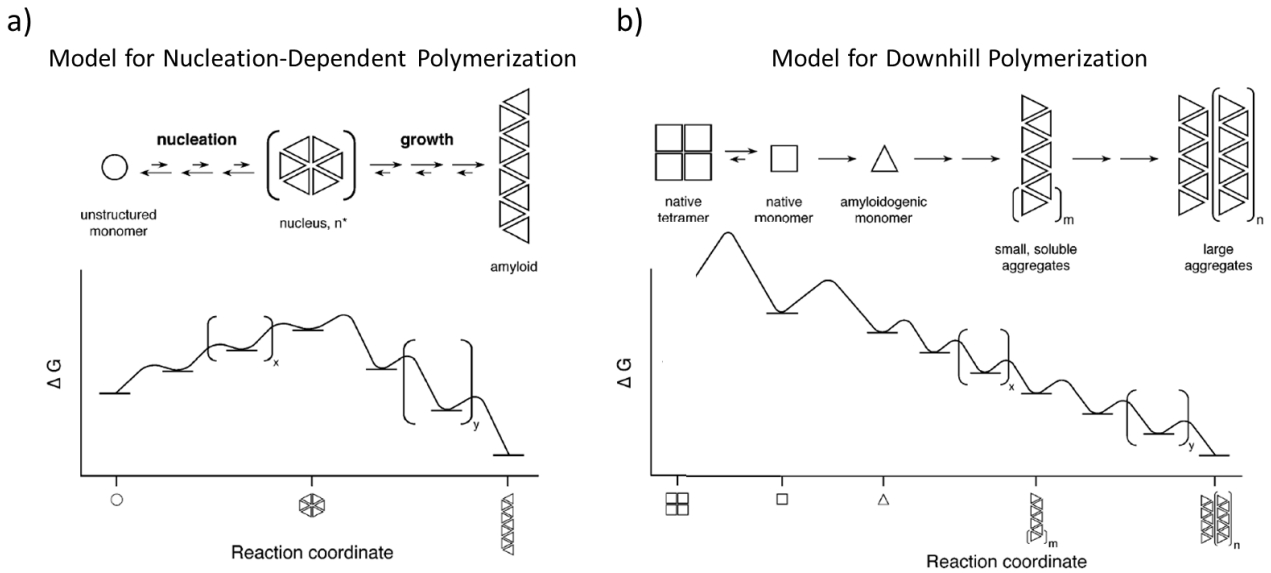

Figure 7. a) and **b)** (Hurshman et al. 2004)

1.2.2 Cytotoxicity of TTR amyloid fibrils

Historically it was assumed that TTR amyloid fibrils cause tissues damage by direct compression, obstruction and local blood circulation failure. However it was also demonstrated that TTR amyloid fibrils are not toxic, whereas monomeric or oligomeric forms of TTR are cytotoxic (Reixach et al. 2004) and it has been suggested that fibrillation intermediates, rather than mature fibrils, could be the pathogenic agents (Haass and Selkoe 2007). Several studies have demonstrated the presence of surface-exposed hydrophobic patches as common feature of oligomers (Bolognesi et al. 2010) that lead to perturbation in the structure of cellular lipid membranes such as disruption of cellular ion homeostasis (Fändrich 2012). It was also reported that lower molecular weight TTR oligomers induced calcium influx via voltage dependent calcium channels (Hou et al. 2007). Moreover, oxidised form of TTR result to be cytotoxic, suggesting that ageing-related oxidative modifications of TTR may contribute to the late-onset of TTR amyloidosis (Zhao, Buxbaum, and Reixach 2013)

1.2.3 Treatment of TTR amyloidosis

Nowadays different therapeutic strategies have been proposed to prevent unfolding or misfolding of TTR with consequent inhibitions of amyloid fibrils formation. For some of these, clinical effectiveness has yet been proven such as liver transplantation or tetramer native state stabilization. Other strategies like Gene Therapy, combination therapy of doxycyclin/tauroursodeoxycholic acid and Immune Therapy, for which interesting results were obtained in the mouse model, have not yet shown clinical effectiveness (**Figure 8**) (Sekijima 2015).

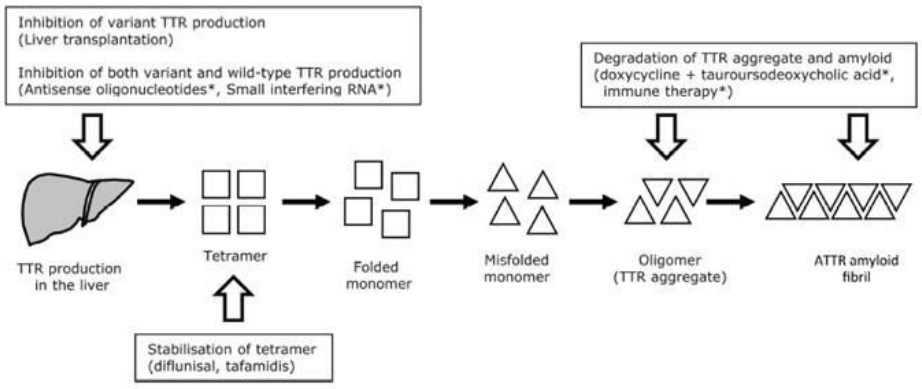

Figure 8. Schematic process of TTR misfolding and aggregation with sites of action of therapeutic strategies (Sekijima 2015)

1.2.3.1 Liver transplantation

The first and widely used therapeutic strategy is liver transplantation. Considering that the 95% of plasma TTR is synthesized by the liver, the net result of liver transplantation is to lower the concentration of amyloidogenic monomers in the blood and thereby to slow disease progression and to extend lifespan. Today, more than 2000 patients were subjected to liver transplantation for these disorders (Ankarcrona et al. 2016). Liver transplantation is the current standard therapeutic strategy for FAP but shows different limitations, including: requirement for surgery, long-term post-transplantation and immunosuppressive therapy. Moreover this kind of strategy is not a viable option for the treatment of acquired amyloidosis and familial leptomeningeal amyloidosis, considering that TTR is also synthesized in retina and in choroid plexus (Sekijima 2015).

1.2.3.2 TTR tetramer stabiliser

Considering that the tetramer dissociation is necessary for TTR amyloid fibril formation, a second therapeutic option for ameliorating TTR amyloidosis is to stabilise the native TTR tetramer structure. Miroy et al. (1996) reported that the binding of T4, the natural TTR ligand, is able to prevent monomer dissociation *in vitro*, but unfortunately the 99% of TTR binding sites in human plasma are unoccupied. Considering that small ligands as T4 can stabilize TTR native state preventing fibril formation, screening experiments (Baures, Peterson, and Kelly 1998, McCammon et al. 2002) and structure-based drug design efforts (Klabunde et al. 2000, Connelly et al. 2010) were made to discover small molecules able to stabilize the TTR tetramer. Nowadays there are only two molecules that passed phase III clinical trials: Diflunisal and Tafamidis. (**Figure 9**).

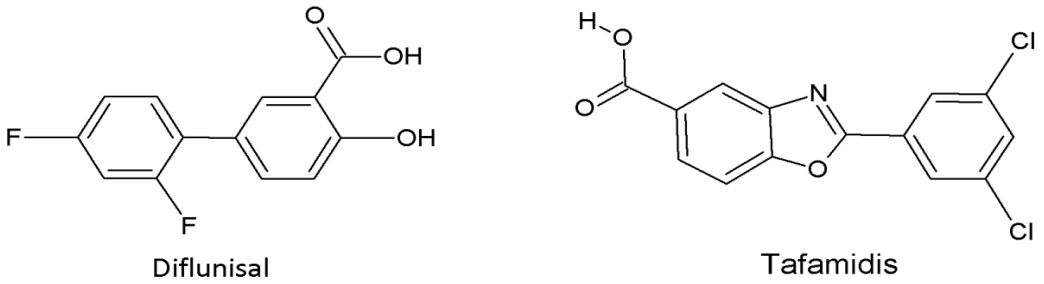

Figure 9.

- Diflunisal: is a nonsteroideal anti-inflammatory drug (NSAID), FDA-approved for the treatment of rheumatoid arthritis and it's a repurposed drug discovered by screening. *In vitro* analysis showed that it is able to bind TTR T4 binding sites (K_{d1}=75nM and K_{d2}=1.1μM) and can inhibit TTR fibril formation (Hammarström et al. 2003, Miller, Sekijima, and Kelly 2004). Moreover, clinical trials showed the ability of Diflunisal to stabilize TTR tetramer of treated patients (Berk et al. 2013). Diflunisal proved to be a good kinetic stabilizer, in particular owing to its high oral bioavailability, (Sekijima, Dendle, and Kelly 2006). Diflunisal is not able to cross the blood brain barrier (Nuernberg, Koehler, and Brune 1991) and it is not suitable for the treatment of leptomeningeal amyloidosis.
- Tafamidis (Vyndraqel®): produced by Pfizer Inc. Tafamidis is a fit-for-purpose TTR stabilizer fashioned by structure-based design developed by Razavi et al. (2003). *In vitro* analysis showed that it is able to bind T4 binding site with better affinity for both sites relative to Diflunisal (K_{d1}=2nM and K_{d2}=154nM) (Bulawa et al. 2012). Clinical trial conducted by Coehlo et al. (2012) showed its ability to lower polyneuropathy progression in patients with FAP. Tafamidis proved to be a good TTR stabilizer in particular owing to its high affinity for TTR binding sites and for its reduced administration dose.

Apart from Tafamidis and Diflunisal there are several other compounds that are not yet approved for the treatment of FAP disease but show stabilizing effect on native TTR structure *in vitro*, *ex vivo* and *in vivo*. Examples of these small ligands are Tolcapone and CSP-1103 (formerly known as CHF5074) (**Figure 10**).

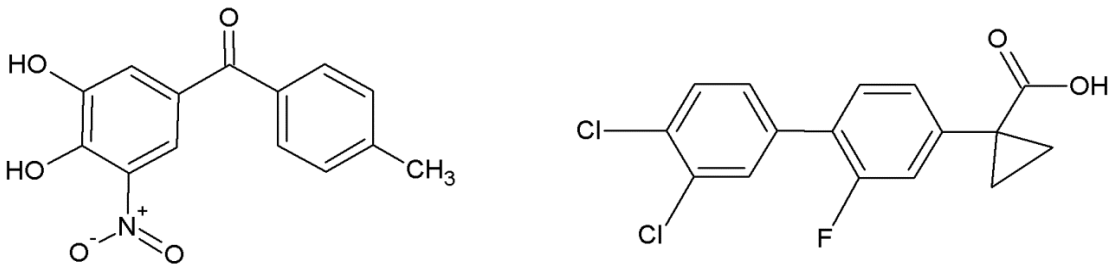

Tolcapone CSP-1103

Figure 10.

- Tolcapone: is a cathecol-O-methyltransferase (COMT) inhibitor authorized in the United States and Europe as an adjunct to levodopa and carbipoda for the treatment of Parkinson's disease (Jorga et al. 1997). Robinson at al. (2014) showed the stabilizing effect of Tolcapone, on TTR native structure, *in vitro*(SOM0226). Sant'Anna et al. (2016) showed

that Tolcapone binds with high affinity and strongly inhibits the aggregation of wt hTTR, hTTR Val122Met (involved in cardiac TTR amyloidosis) and hTTR Ala25Thr(involved in leptomeningeal amyloidosis). Moreover it is able to stabilize TTR *ex vivo* and *in vivo*. The only limitation of Tolcapone which compared to Diflunisal and Tafamidis is the shorter half-life(~ 2-3h). Currently, Tolcapone is in phase II clinical trial for the treatment of FAP diseases (Clinical trials.gov Identifier: NCT02191826/Eudra CT number: 2014-001586-27).

- CSP-1103: it has been shown that some nonsteroideal anti-inflammatory drugs (NSAIDs) decrease the production of Aβ42 *in vitro* and *in vivo* (Weggen et al. 2001; Gasparini et al. 2004) and counteract the progression of Aβ42 pathology in transgenic mouse model of Alzheimer's disease (Lim et al. 2000; Van Groen and Kadish 2005). CSP-1103, formerly known as CHF5074, is a chlorinated derivate of the NSAID Flurbiprofen lacking the cyclooxygenase inhibitory activity, initially developed for the therapy of Alzheimer's disease by Chiesi Farmaceutici S.p.a. (Peretto et al. 2005). Recent studies have also shown the ability of CSP-1103 to interact with TTR stabilizing its tetrameric structure *in vitro* (Zanotti et al. 2013) and *in vivo* (Mu et al. 2015). CSP-1103 is also able to cross the blood-brain barrier (Mu et al. 2015) and, therefore is potentially suitable for the treatment of leptomeningeal amyloidosis.

1.2.3.3 Gene Therapy

Gene silencing approaches using antisense oligonucleotides (ASOs) (Benson et al. 2006; Benson et al. 2010; Ackermann et al. 2012;)or small interfering RNAs (siRNAs) (Coelho et al. 2013) are promising therapeutic agents for the amelioration of wt TTR amyloidosis.

- Antisense oligonucleotides (ASOs): are short modified oligonucleotides designed to prevent protein translation by selectively binding to the complementary RNA in cells. Benson et al. (2006) identified TTR specific ASOs able to suppress serum TTR protein levels in transgenic mice carrying human Ile84Ser TTR. Subsequently Isis Pharmaceutical developed ISIS-TTR_{RX}, which binds to the 3' portion of the human TTR mRNA (Ackermann et al. 2012).
- Small interfering RNA (siRNAs): are 21-23 nucleotides long double-stranded RNA molecules able to target and to cleave complementary mRNA. Alnylam Pharmaceutical Inc developed several TTR-specific siRNA formulations. An example is provided by ALN-TTR02, an anti-TTR siRNA encapsulated in a second-generation formulation of lipid nanoparticles (Coelho et al. 2013).

1.3 Transthyretin (TTR) and hydroxyisourate hydrolase (HIUase)

1.3.1 Uric acid degradation pathway and pathological implications

Uric acid is the final product of purine catabolism, derived from the enzymatic reaction of Xanthine oxidoreductase. Many organisms share the ability to degrade uric acid into more soluble compounds through three enzymatic reactions (**Figure 11**). The reaction is initiated by urate oxidase which coverts uric acid into 5-hydroxyisourate (5-HIU), an unstable compound that decomposes spontaneously to 2-oxo-4-hydroxy-4-carboxy-5-ureidoimidazoline (OHCU) and subsequently into Aallantoin. 5-hyroxyisourate hydrolase (HIUase) catalyses the hydrolysis of 5-HIU into OHCU that is converted in turn by OHCU decarboxylase to S-(+)-Allantoin (Ramazzina et al. 2006).

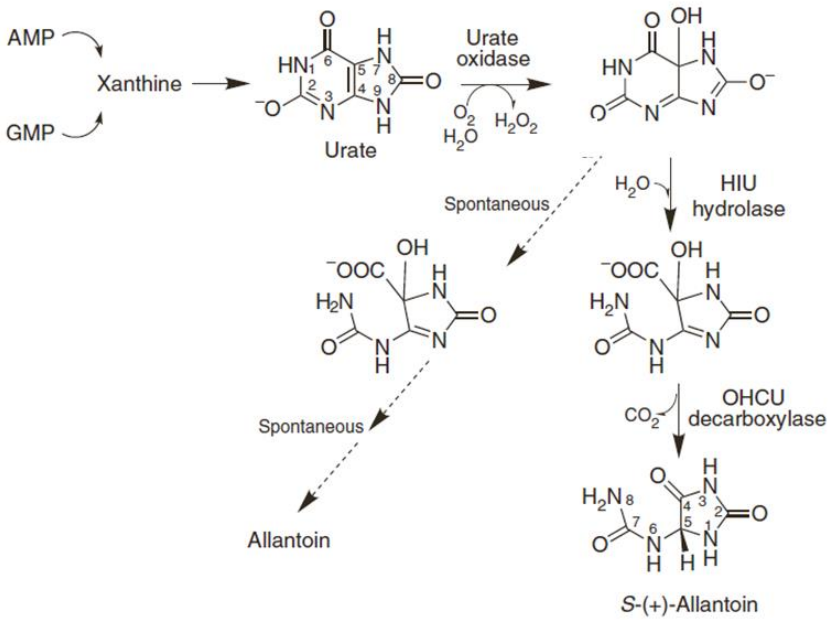

Figure 11. Uric acid degradation pathway (Ramazzina et al. 2006)

This pathway has been lost or gained several times during evolution, in fact human and apes together with other organisms share the inability to degrade uric acid (Ramazzina et al. 2006). The absence of this pathway, but in particular the inactivation of urate oxidase that occurred in a primate ancestor 15 million years ago, lead to the increase of uric acid level in plasma (Oda et al. 2002). Humans can develop hyperuricemia, a pathology characterized by crystallization and deposition of uric acid in joints and surrounding tissues (Gliozzi et al. 2016). The uric acid level can be enhanced by over production (Lesch and Nyhan 1964) or lowered excretion (Graessler et al. 2006; Brandstatter et al. 2008) of uric acid. Currently the long-term management of hyperuricemia

is aimed at modulating the activity of key proteins involve in the metabolism and excretion of uric acid. They are divided in two main classes:

- Uricostatic drugs: which reduce uric acid production through competitive inhibition of xanthine oxidase, such as Allopurinol and Febuxostat.
- Uricosuric drugs: which increase urinary uric acid excretion by blocking renal tubular reabsorption of urate, such as Probenecib.

Patient refractory to conventional treatments may be treated with Pegloticase, a pegilated pig-baboon urate oxidase. Pegloticase can only be use over a short period (3-6month) because many patients often develop anti-pegloticase antibodies that can reduce the efficacy of the pegilated enzyme (Gliozzi et al. 2016).

1.3.2 Similarity between TTR and HIUase

5-hydroxyisourate hydrolase (HIUase) the second enzyme of the uric acid degradation pathway share a high degree of amino acid sequence similarity (approximatively 50%) with TTR (Zanotti et al. 2006) and a highly conserved fold with TTR, as revealed by X-ray analysis of both bacterial (Hennebry et al. 2006; Jung et al. 2006; French and Ealick 2011) an vertebrate (*Danio rerio*) HIUases (Cendron et al. 2011; Zanotti et al. 2006). The similarity of these proteins can be ascribed to a duplication event in the gene encoding HIUase, which gave rise to TTR at a very early stage of vertebrate evolution; gene duplication backdate to before the separation of *Agnatha*, over 530 milion years ago (Zanotti et al. 2006). The long channel that transverse both tetramers of HIUases and TTR was affected by the major evolutionary changes. TTR channel is deep and negatively charged and harbors two binding sites for the thyroid hormone molecules, while in HIUase the channel is shallower, positively charged and the enzyme active sites occupy only a portion of the thyroxine binding cavities of TTR. Cendron et al. (2011) demonstrated that two residues replacement (Tyr→Thr and Ile→ Ala) in the *Danio rerio* HIUase active site are able to open up the two ends of the channel, generating two cavities accessible to the thyroxine molecule, abrogating at the same time the enzymatic activity.

1.3.3 HIUase mechanism of action

Several mutagenic studies have been conducted on different bacterial HIUases in order to understand their mechanism of action (Hennebry et al. 2006; Jung et al. 2006; French and Ealick 2011). Considering the lack of a strong nucleophile in the active site, such as glutamate, it has

been hypothesized that the reaction is likely to be initiated by a water molecule that requires activation by deprotonation. Different works suggested that the major residues involved in the catalysis are two histidines. The mechanism of action, proposed by using the *Klebsiella pneumoniaea* model, is shown in **Figure 12.**

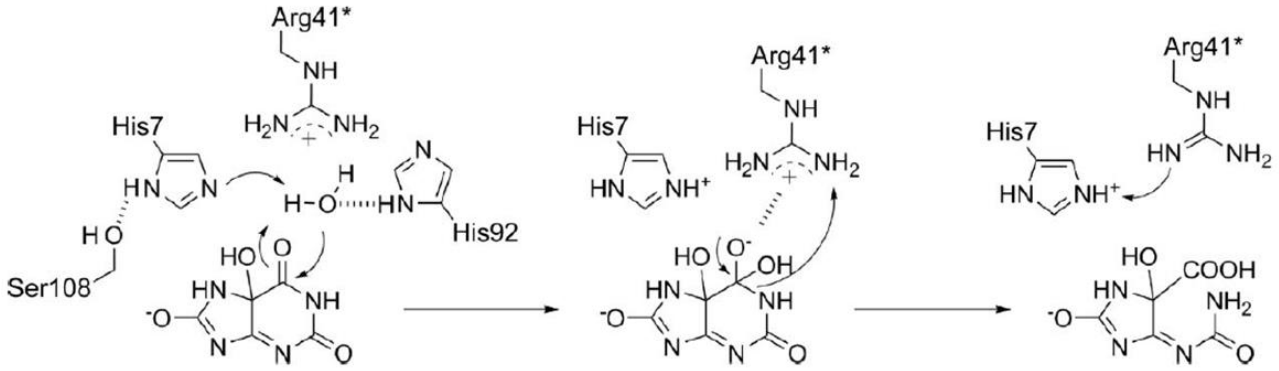

Figure 12. Mechanism proposal for the conversion of 5-HIU to (S)-Allantoin by *Klebsiella pneumoniaea* HIUase (French and Ealick 2011)

The two histidines His7 andHis92 in the active site are responsible for water deprotonation, in order to generate a hydroxide nucleophile necessary for the nucleophile attack, and for the orientation of the water ideally for attack at C6 of the purine ring, respectively. The highly conserved Ser108 at C-terminus is positioned to form a hydrogen bond with His 7 and may indirectly participate in catalysis by inductively activating this residue. The charge on the resulting oxyanion would be stabilized by the positively charged guanidinium group of Arg41. Collapse of the oxyanion would then lead to ring opening. The original proton abstracted from a water molecule by His7 would then be transferred to Arg41 to complete the catalytic cycle (French and Ealick 2011).

1.4 Retinoids and Retinoid Binding Proteins (RBPs)

Retinoids are a class of compounds chemically related to Vitamin A. Structurally they are composed by three distinct domains: a β-ionone ring, an isoprenoid tail consisting of four isoprenoid units joined head-to-tail and a polar end-group such as hydroxyl end-group (retinol), aldehyde end-group (retinal) or carboxylic moiety (retinoic acid) (**Figure 13**) (Sporn et al. 1976). This definition of retinoids include both the natural forms or synthetic analogs of retinol, with or without biological activity. Sporn and Roberts (1985) proposed another definition for retinoids in order to include synthetic compounds that do not show the structural or chemical similarity with retinoids but show a biological activity similar to that of vitamin A. Regarding the physiological

roles, vitamin A and its derivtatives are essential in a great number of biological process such as: vision, immune function, reproduction, maintenance of epithelial tissue and embryonic development. One of the best characterized bioactive metabolites of vitamin A, 11-cis-retinal, is critical for the visual function. 9-cis-retinoic acid, is a potent regulator of gene transcription, plays important roles in regulating cell proliferation and differentiation (**Figure 13**) (Blomhoff and Blomhoff 2006).

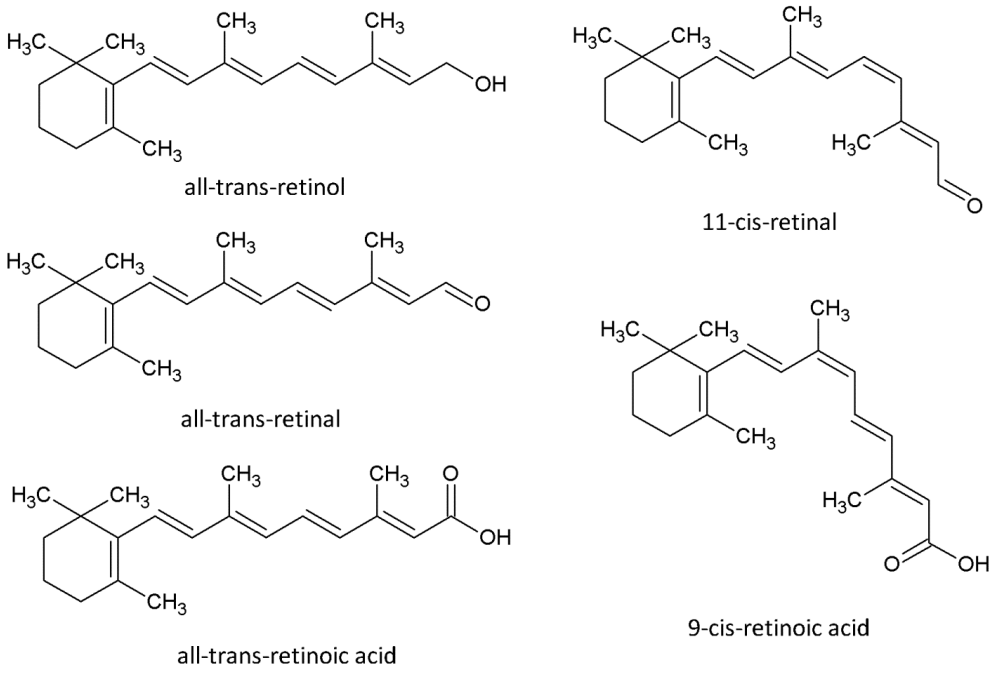

Figure 13.

1.4.1 Retinoid binding proteins

Retinol is a chemically unstable and quite insoluble compound in the aqueous medium. The interaction with distinct intracellular and extracellular transport proteins, in order to protect and solubilize it, appears to be crucial (Zanotti and Berni 2004). These carrier proteins are known as retinoid binding proteins and belong to two protein families that were classified as transport proteins for hydrophobic compounds: the lipocalins and the intracellular lipid-binding proteins (iLBPs). RBP belongs to the lipocalin superfamily, designated with this name, owing to the fact that their structure has the shape of a calyx, provided by β-barrel a The members of this family possess diverse functions and are characterized by a highly conserved structural motif, despite the low degree of sequence identity. RBP is a single-domain protein of approximatively 21KDa, made up of eight antiparallel β-strand, denoted A-H, which form a β-barrel and a short α-helix close to the C-terminus (**Figure 14**)(Zanotti et al. 1993).

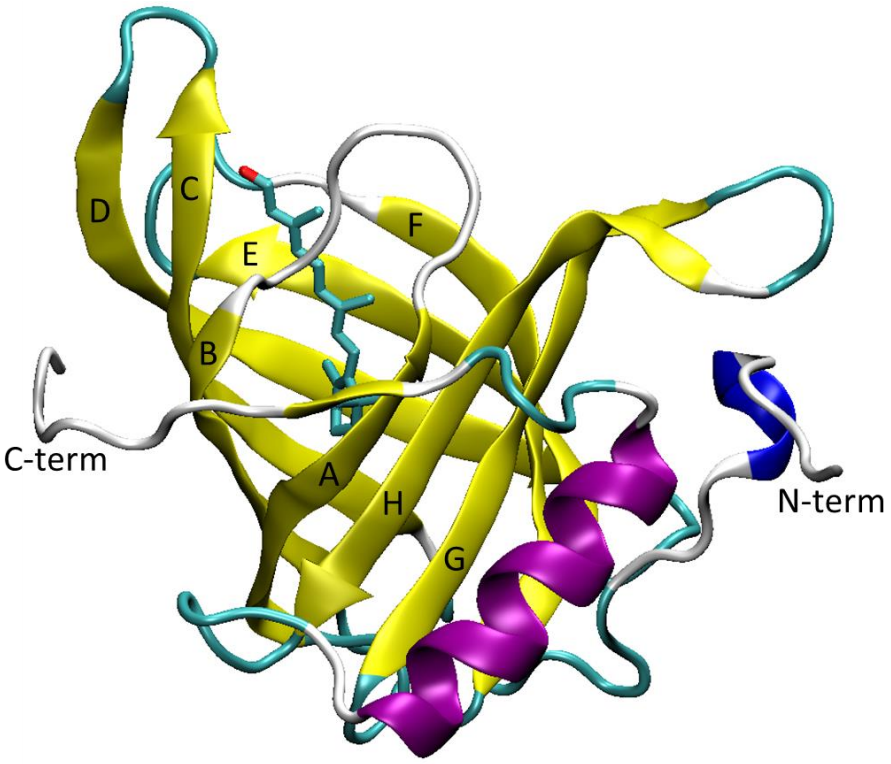

Figure 14. Ribbon depiction of retinol-RBP complex

The retinol is deeply buried in the cavity where the cyclohexene ring point toward the bottom of the calyx and the polyene chain is fully extended and substantially planar. The open end of the β-barrel consist of three loops encompassing residues between strand A-B, C-D and E-F that are close to the retinol hydroxyl end group and define the ligand entrance. A fourth loop encompassing residues between strand G-H is located far from the ligand. The interactions of the retinol within the cavity are mainly hydrophobic. The hydroxyl end group of retinol establishes polar interactions with RBP participating in two H-bond interactions with the main chain N atom of Gln98 and with O atom of Phe96, involving a H-bond water bridge. Moreover a network of H-bond in addition to hydrophobic interactions appears to stabilize the binding of retinol (Zanotti et al. 1993).

1.4.2 Differences between apo-RBP and holo-RBP

The superposition of apo and holo models of RBP, represented in **Figure 15.a**, shows a great degree of similarity between the two structures. However the apo-holo comparison reveals a protein conformational change in the region encompassing amino acids in the A-B loop, where a twisting of the corresponding portion of the main chain lead to a different orientation of the side chains of Leu35 and Phe36. As a result Phe36 occupies some of the space left from the vitamin while Leu35 moves out of the binding site pointing toward the exterior of the protein (Zanotti et

al. 1993). Considering that Leu35 is one of the main residues of RBP involved in the recognition of TTR (Monaco, Rizzi, and Coda 1995), the conformational change of the A-B loop may be linked to the different affinity of apo and holo RBP for TTR (Zanotti et al. 1993). In **Figure 15.b** and **c** the different position of side chain of Phe36 and Leu35, respectively, are shown in a superposition representation of apo and holo RBP.

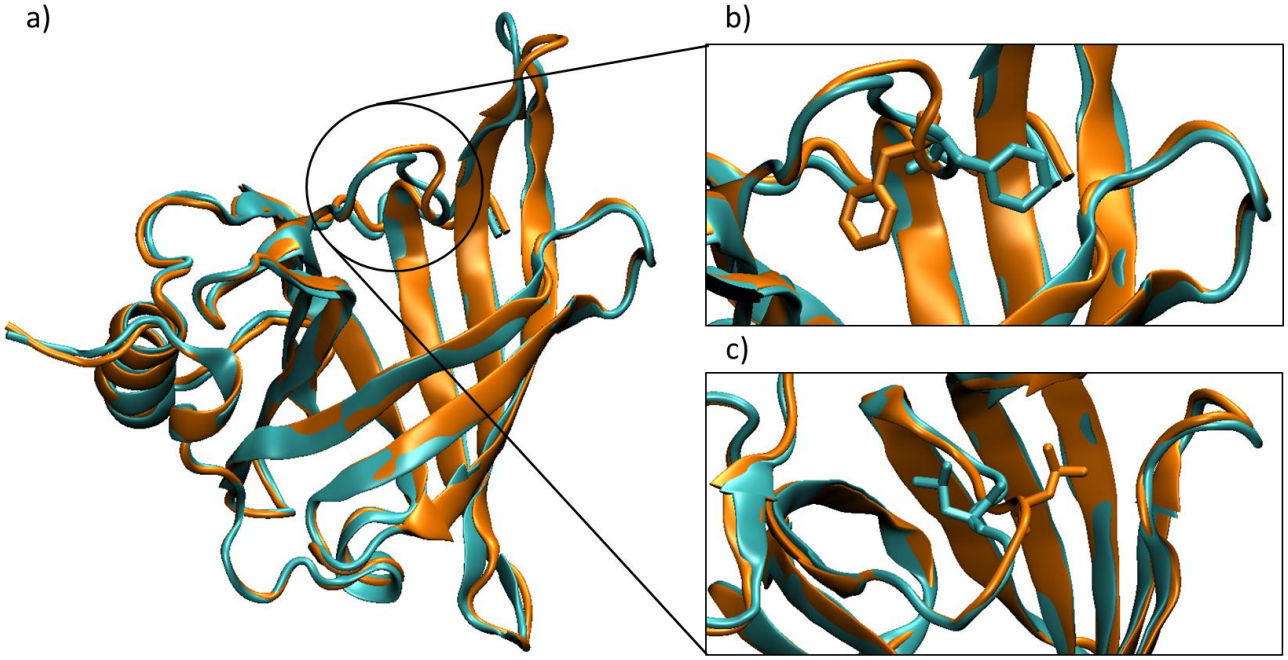

Figure 15. a) superposition representation of apo-RBP (cyan) and holo-RBP (orange), **b)** Superposition representation of side chain of Phe36, **c)** Superposition representation of side chain of Leu35

1.4.3 RBP mutant forms and pathological implications

Due to the involvement of vitamin A in different important biological processes low levels of vitamin A have been found to be associated with different diseases. Vitamin A deficiency (VAD) are mainly related to visual disorders, such as night blindness (nyctalpia), a reversible loss of visual adaptation to dark environment (Dowling and Wald 1958). Considering that vitamin A is a substrate for the synthesis of retinoic acid, a signalling molecule needed for vertebrate organogenesis (Duester 2009), different studies have associated maternal vitamin A deficiency with eye malformations and urogenital, diaphragmatic, cardiovascular, and pulmonary defects (Wilson, Roth, and Warkany 1953; See and Clagett-Dame 2009). Further, more mutations in the retinol membrane receptor STRA6, cause autosomal recessive anophtalmia or Matthew-Wood syndrome, characterized by structural eye defects, diaphragmatic hernias, cardiac malformation and pulmonary hypoplasia (Chassaing et al. 2009; Casey et al. 2011;). Pathologies related to

vitamin A deficiency are also associated with retinol binding protein mutations. For example mutations I41N and G75D found by Biesalski et al. (1999) are associated with night blindness and very low plasma retinol and RBP concentrations. Folli et al. (2005) showed that these holo-RBP mutant forms are able to interact normally with TTR but possess a low affinity for retinol. These data indicate that the lower plasma retinol concentration may be due to an enhanced retinol release and as a consequence an accelerated filtration of uncomplexed apo-RBP, through kidney glomeruli. Recently Chou et al. (2015) identified other two missense mutations (A55T and A57T) in the RBP gene, associated with congenital eye malformation, microphtalmia, anophtalmia and coloboma (MAC) disease. They demonstrated that these two RBP mutant variants are stably secreted and interact normally with TTR. Both RBP mutants are able to interact with retinol but show a higher release of the vitamin (A55T>A57T>wt) when exposed to ethanol, detergents and phospholipid vesicles. Furthermore, the evaluation of RBP-STRA6 interaction revealed a higher affinity for the receptor. Chou et al. (2015) suggested that A55T and A57T mutations may exist in a partially melted state under physiological conditions, that resemble wt intermediates in the RBP-STRA6 binding reaction, enhancing binding of mutant RBP to STRA6.

MATERIALS AND METHODS

2.1 Growth medium and antibiotics

Lysogen broth (LB) was prepared in ddH2O by adding all the components (Formedium), at the final concentrations reported in the table below . If necessary, agar was added to the growth medium at the final concentration of 1.5% (p/v). Sterilization of all preparation were performed in autoclave for 20min at 121°C.

Component	**Final Concentration**
Trypton	1% (p/v)
Yeast Extract	0.5% (p/v)
Sodium Chloride	1% (p/v)

In order to select *Escherichia coli* strains and expression vectors, antibiotics (Sigma-Aldrich) were added to lysogen broth at the final concentrations reported in the table below.

Antibiotic	**Final Concentration**
Ampicillin	100µg/ml
Chloramphenicol	34 µg/ml
Tetracycline	10µg/ml

2.2 Bacterial strains

***Escherichia coli* XL1-Blu competent cells**

XL1-Blu strain allows blue-white color screening for recombinant plasmids and is an excellent strain for routine cloning applications. These cells are endonuclease (*endA*) deficient, which greatly improves the quality of miniprep DNA and the *hsdR* mutation prevents the cleavage of cloned DNA by the EcoK endonuclease system. The *lacI* gene on the F' episome allows blu-white color screening. Further the F' episome contains tet^R gene that ensure tetetracycline resistance.

***Escherichia coli* BL21-Codon Plus competent cells**

BL21- Codon Plus strain expresses T7 RNA polymerase under control of an operon lac and allows efficient high-level expression of heterologous proteins. Efficient production of heterologous protein in *Escherichia coli* is frequently limited by the rarity of certain tRNAs that are abundant in the organism from which the proteins are derived. Forced high-level expression of heterologous proteins can deplete the pool of rare tRNAs and stall translation. BL21-Codon Plus cells are engineered to contain extra copies of genes that encode the tRNAs that most frequently limit

translation, localize on a vector that contains *cam*^{R} gene that ensure chloramphenicol resistance. Moreover this strain is deficient in *lon* and *ompT* genes coding for two proteases.

2.3 Expression vector

pET11-b

The expression of all heterologous protein were carried out using the pET11-b expression vector show in **Figure 16**. The pET11-b expression vector, derived from the pBR322 plasmid, is engineered to take advantage of the features of the T7 bacteriophage gene promoter that allows high level transcription and translation. The vector contains *lacI* gene and *amp*^{R} gene that confer ampicillin resistance in order to select correctly transformed cells.

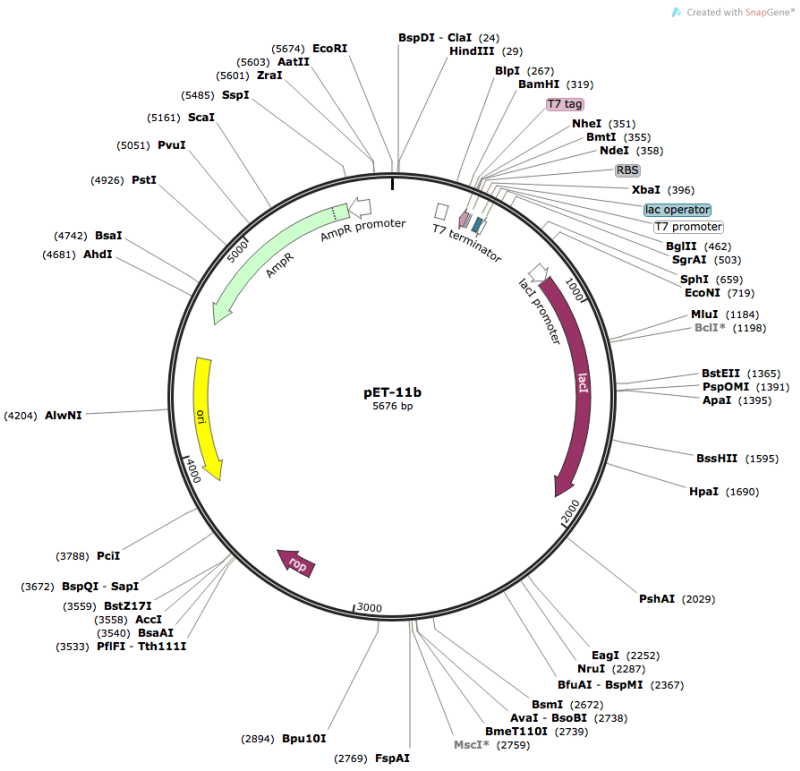

Figure16. Genetic map of pET11-b

2.4 TTR and RBP site directed mutagenesis

All mutant forms of human transthyretin (hTTR) and human retinol binding protein (hRBP) were obtained by Quick change site-directed mutagenesis. The mutagenic oligonucleotide primers (**Table 4**) were designed according to the following parameters and purchased from BMR Genomics:

- length between 25 to 45 bases and the desired mutation in the middle of the primer with 10-15 bases of correct sequence on both sides
- minimum GC content of 40% and one or more C o G bases at the end
- melting temperature (T_m) greater or equal to 78°C. The calculation of T_m was performed using the following equation that consider the % mismatch where N is the primer length in bases and %GC and %mismatch are whole numbers.

$$T_m = 81.5 + 0.41(\%GC) - 675/N - \%mismatch$$

Primer	**Sequence**
hTTR K15H Forward	5′-GTGTCCTCTGATGGTCCACGTTCTAGATATTGTCCGAG-3′
hTTR K15H Reverse	5′-CTCGGACAATATCTAGAACGTGGACCATCAGAGGACAC-3′
hTTR A19I Forward	5′-TGGTCAAAGTTCTAGATATTGTCCGAGGCAGTCCTGCC-3′
hTTR A19I Reverse	5′-GGCAGGACTGCCTCGGACAATATCTAGAACTTTGACCA-3′
hTTR A25T Forward	5′-CCGAGGCAGTCCTACCATCAATGTGGCC-3′
hTTR A25T Reverse	5′-GGCCACATTGATGGTAGGACTGCCTCGG-3′
hTTR E54R Forward	5′-ACCAGTGAGTCTGGACGGCTGCATGGGCTCAC-3′
hTTR E54R Reverse	5′-GTGAGCCCATGCAGCCGTCCAGACTCACTGGT-3′
hTTR T106H Forward	5′-CCCCGCCGCTACCACATTGCCGCCCTG-3′
hTTR T106H Reverse	5′-CAGGGCGGCAATGTGGTAGCGGCGGGG-3′
hTTR T119Y Forward	5′-CCCTACTCCTATTCCACCTATGCTGTCGTCACCAATCCCA-3′
hTTR T119Y Reverse	5′-TGGGATTGGTGACGACAGCATAGGTGGAATAGGAGTAGGG-3′
hRBP A55T Forward	5′-GCCAGATGAGCACCACAGCCAAGGGC-3′
hRBP A55T Reverse	5′-GCCCTTGGCTGTGGTGCTCATCTGGC-3′
hRBP A57T Forward	5′-ATGAGCGCCACAACCAAGGGCCGAGTC-3′
hRBP A57T Reverse	5′-GACTCGGCCCTTGGTTGTGGCGCTCAT-3′

Table 4. Primer used in the mutagenesis reaction

Site directed mutagenesis reaction was performed in a final volume of 50µl, using 30ng of DNA template (pET11-b hTTR wt or pET11-hRBP wt), 125ng of each oligonucleotide primers designed as mentioned above, and 2.5U of PfuTurbo DNA polymerase (Promega) by using Mastercycler (BIO-RAD). The cycling parameters for the amplification are reported below:

Number of Cycles	Temperature	Time
1	95°C	30 seconds
12	95°C	30 seconds
	55°C	1 minute
	68°C	12 minute (2minutes/Kb)

At the end of the amplification, the reaction was cooled in ice for 2 minutes to reach a temperature below 37°C. Selection of neo-synthesized plasmid containing the desire mutation was performed by digestion with 1U of DpnI (New England Biolabs) for 2h at 37°C, in order to remove parental DNA template. After DNA precipitation (1/3 volume reaction of 96% Ethanol, 1/10 volume reaction of 3M Sodium Acetate) for 16h at -20°C the digestion product was dissolved in 3µl H_2O MilliQ and half preparation was used to transform XL1-Blu competent cells by electroporation using Micropulser (BIO-RAD). Transformed cells were plated on lysogen broth supplemented with Ampicillin and Tetracycline. After 16h incubation at 37°C, selected clones were subjected to minipreparation of plasmid DNA using a kit purchased by Fisher Molecular Biology (FMB). The correct insertion of the mutation on hTTR or hRBP gene was evaluated by sequencing using the service provide by BMR Genomics.

2.5 Expression of recombinant proteins

The expression of all heterologous proteins were performed by means of T7 expression system using BL21-CodonPlus competent cells conveniently transformed with pET11-b expression vector containing the gene encoding for hTTR or hRBP, wt or mutant forms.

2.5.1 hTTR wt or mutant forms expression

Transformed BL21-CodonPlus strain were grown in 1L of lysogen broth supplemented with Ampicillin and Chloramphenicol at 37°C up to an absorbance value at 600nm between 0.6OD and 0.8OD. The expression of recombinant protein was achieved by induction with isopropyl β-D-1-thiogalactopyranoside (IPTG) at the final concentration of 1mM and incubations at 30°C for 4hour. Samples before and after induction was subjected to SDS-PAGE to evaluate the successful expression of heterologous protein. Cells were harvested using a refrigerated centrifuge SL 40 FR (Thermo Fisher) at 7000rpm for 10minutes, than washed with TE buffer (50mM Tris HCl, 1mM EDTA pH8.0) and centrifuged again. Cells were subsequently resuspended in 60ml of lysis buffer (50mM NaP, 300mM NaCl, 10% (v/v) Glicerol pH 8.0) and subjected to 40 cycles of sonication of 30seconds and 1minutes of rest in ice, using a Sonicator 300 (Misonix). The supernatant was separated from insoluble fraction by centrifugation at 10000rpm for 20min. The successful sonication was evaluated by SDS-PAGE. Supernatant was concentrated up to 10ml in AMICON (membrane cutoff 10KDa) and dialysed against 2L of 30mM Tris HCl pH7.5.

2.5.2 hRBP wt or mutant forms expression

Transformed BL21-CodonPlus strain were grown in 1L of lysogen broth supplemented with Ampicillin and Chloramphenicol at 37°C up to an absorbance value at 600nm between 0.6OD and 0.8OD. The expression of recombinant protein was achieved by induction with isopropyl β-D-1-thiogalactopyranoside (IPTG) at the final concentration of 1mM and incubations at 37°C for 16hour. Samples before and after induction was subjected to SDS-PAGE to evaluate the successful expression of heterologous protein. Cells were harvested using a refrigerated centrifuge SL 40 FR (Thermo Fisher) at 7000rpm for 10minutes, than washed with TE buffer (50mM Tris HCl, 1mM EDTA pH8.0) and centrifuged again. Cells were subsequently resuspended in 60ml of lysis buffer (50mM NaP, 300mM NaCl, Glicerol 10% (v/v) pH 8.0) and subjected to 40 cycles of sonication of 30seconds and 1minutes of rest in ice, using a Sonicator 300 (Misonix). The supernatant was separated from insoluble fraction by centrifugation at 10000rpm for 20min. The recombinant RBP, which was present in the insoluble fraction, need to be unfolded and refolded in order to be purified. To achieve this result a modified protocol designed by Xie et al. (1998) was used. Insoluble fraction was dissolved in 20ml of 8M urea then diluted to 6.5M urea after addition of 2.6ml of 25mM Tris HCl pH 9.0. Then the sample was diluted 4 fold with 6.5 M urea and the pH adjusted to 9,0. To achieve reduction and further solubilization, β-mercaptoethnol (Sigma Aldrich) was added to the suspension at the final concentration of 20mM, prior incubation for 16h at 24°C with vigorous mechanical stirring. The successful sonication and unfolding was evaluated by SDS-PAGE. Protein refolding was achieved by 5 fold dilution of the unfolded protein in the refolding oxidative buffer (25mM Tris HCl, 0.3mM Cystin, 3mM Cystein, 1mM EDTA pH 9.0) and in the presence of 10mg of retinol (Sigma Aldrich) dissolved in ethanol. All solutions were prechilled in a cold room and the refolding was achieved after at least 5h incubation at 4°C with vigorous mechanical stirring. Supernatant was concentrated up to 10ml in AMICON (cutoff 10KDa) and dialysed against 2L of 30mM Tris HCl pH7.5.

2.6 Protein purification

All heterologously expressed protein were purified with two chromatographic steps: anion exchange and size exclusion chromatography. After these purification steps TTRs were subjected to hydrophobic interaction chromatography while RBPs were subjected to affinity chromatography using a TTR functionalized matrix.

2.6.1 Anion Exchange chromatography

After dialysis, all proteins extracts were concentrated up to 5ml in AMICON and purified by anion exchange chromatography using 30ml of Macro-Prep High Q support matrix (GE Healthcare) and taking advantage of the Äkta Plus system (GE Healthcare). The matrix was previously equilibrated with 3 volumes of 30mM Tris HCl pH 7.5 prior sample loading. A constant flow rate of 0.6ml/min was applied to the column and proteins were eluted with a linear NaCl gradient from 0M to 0.5M. The resulting fractions (3ml) were subjected to absorbance analysis at 280nm to monitor the elution profile. Fractions were further analyzed by SDS-PAGE. Selected fractions were combined and concentrated in a Centricon cell (membrane cutoff of 10KDa) up to 1ml volume and submitted to the next chromatographic step.

2.6.2 Size exclusion chromatography

After anion exchange chromatography, selected fractions were subjected to size exclusion chromatography using 100ml of Ultrogel AcA 54 matrix (PALL Life Science). The separation range from 70KDa to 5KDa of the matrix is suitable for purification of hTTR (approx. 55KDa) or hRBP (approx. 21KDa). The purification was performed in 50mM Tris HCl, 100mM NaCl pH 7.5 keeping a flow rate of 0.2ml/min. Resulting fractions (2ml) were subjected to absorbance analysis in order to monitor the elution profile. Fractions were further analyzed by SDS-PAGE. Selected fractions were combined and concentrated in a Centricon cell (membrane cutoff 10KDa) up to 1ml and submitted to the next chromatographic step.

2.6.3 Hydrophobic interaction chromatography

Hydrophobic interaction chromatography was performed to purify wt or mutated TTR. After size exclusion chromatography, to the pool of selected and concentrated fractions, ammonium sulfate was added to a final concentration of 0.8M, and the protein solution was applied to a Phenyl Sepharose 6 Fast Flow (GE Healthcare) column previously equilibrated with 3 volumes of 30mM Tris HCl, 0.8M ammonium sulfate pH 7.5. Proteins were eluted at a flow rate of 0.4ml/min, applying an ammonium sulfate gradient from 0.8M to 0M. After absorbance and SDS-PAGE analysis, selected fractions containing purified protein were concentrated and protein quantified spectrophotometrically at 280nm as described below, stored at -20°C.

2.6.4 TTR-affinity chromatography

TTR-affinity chromatography was performed for the purification of wt and mutant hRBP. This type of chromatography is based on TTR-RBP specific interactions, using a matrix consisting of NHS pre-activated Sepharose 4B resin (Sigma Aldrich), specifically functionalized with wt hTTR, according to the provided protocol. RBP fractions lacking affinity for TTR were eluted from the column in the presence of the equilibrating buffer (50mM NaP, 150mM NaCl pH 7.5), whereas correctly folded RBP possessing affinity for TTR was retained and could be eluted from the column in an elution step accomplished at low ionic strength. 2 molar equivalents of retinol (Sigma Aldrich) were added to 1mg of refolded hRBP prior loading to the affinity column. The protein was eluted from the column using a decreasing NaP gradient. Collected fractions (0.6ml) were analyzed spectrophotometrically to follow the elution profile. For all fraction the ratio of absorbance at 280nm and 330nm was calculated. Only fraction with an approximate ratio of 1:1, typical of a correctly folded RBP (Xie et al. 1998), were selected, pooled and concentrated in Vivaspin 500 (membrane cutoff 10KDa), and the purified protein, quantified spectrophotometrically at 280nm as described below.

2.7 Enzymatic assay

To evaluate the hydroxyisourate hydrolyse activity of hTTR mutant forms, enzyme assay were performed using a modified method of Lee et al. (Lee et al. 2005). 1µM Uricase (Sigma Aldrich) was added to a solution containing 50mM KP pH7.4, and 50µM uric acid (Sigma Aldrich). The formation of 5-hydroxyisourate by uricase was monitored spectrophotometrically following the increase in absorbance at 312nm. When the absorbance reached the maximum value (approximately after 1min) 2µM of mutated TTR or 2nM *Danio rerio* HIUase were added. The 5-HIU degradation was monitored by following the decrease in absorbance at 312nm.

2.8 Stabilization of TTR tetramer

CSP-1103 and Tafamidis were synthesized according to reported reference respectively (Mu et al., 2015, Bulawa et al., 2012), Diflunisal and Flurbiprofen were purchased by Sigma Aldrich. All drugs were dissolved in DMSO.

2.8.1 Analysis of recombinant TTR stabilization

The stabilizing effect of tested molecules on the wt hTTR and hTTR A25T native state was evaluated in the presence of high concentrations of urea. 10µM wt hTTR in 10mM NaP, 150mM NaCl pH 7.4 was supplemented with DMSO or with 2 molar equivalents of tested compounds (CSP-1103, Tafamidis, Diflunisal and Flurbiprofen). After 1 hour incubation at room temperature, urea was added to the samples to a final concentration of 5M and the mixtures were further incubated at 4°C for 24 hour. TTR was then cross-linked in the presence of 2.5% glutaraldehyde (Pullakhandam et al. 2009) and samples were finally subjected to SDS-PAGE. The images were recorded by using a densitometer (GS-800, BIO-RAD). The experiments were carried out in triplicate and the extent of protection of TTR in the presence of the denaturing agent was revealed by estimating the quantity of protein monomer for each sample in comparison with that present in the sample of TTR devoid of ligands.

2.8.2 Analysis of plasma TTR stabilization

Stabilization experiments in the presence of urea were also conducted for TTR present in human plasma with two different methods**.**

First Method: plasma aliquots were supplemented with increasing concentrations (7.5, 15 and 30 µM) of CSP-1103, Tafamidis, Diflunisal or Flurbiprofen. One more sample containing plasma supplemented with DMSO was prepared as negative control. After 3 hour incubation at room temperature, urea was added up to a final concentration of 6 M. The incubation was prolonged overnight at 4°C for 24h. TTR was then cross-linked in the presence of 2.5% (v/v) glutaraldehyde and finally subjected to SDS-PAGE. The experiments were carried out in triplicate.

Second Method: plasma aliquots were supplemented with increasing concentrations (7.5, 15 and 30 µM) of CSP-1103, Tafamidis, Diflunisal or Flurbiprofen. One more sample containing plasma supplemented with DMSO was prepared as negative control. After 2 hour incubation at room temperature, urea was then added up to a final concentration of 4M. The incubation was prolonged overnight at 4°C for 18h and followed by SDS-PAGE at low SDS concentration (0.86mM) that prevent re-association of TTR monomer but do not denature TTR tetramer (Nilsson et al. 2016). The experiments were carried out in triplicate.

In both procedures protein gels were blotted using Trans-Blot SD transfer apparatus (BIO-RAD) and the membrane were incubated in blocking buffer solution containing 5% (p/v) Skin Milk at 25°C, over-night. Immunodetection of TTR species was performed by employing rabbit anti-human prealbumin polyclonal Ab (Dako) diluted 1:140 and a secondary antibody anti-rabbit IgG labeled with Dylight 680 diluted 1:13000. The images were recorded by using Odissey Image System (LI-COR) and the extent of protection of TTR in the presence of the denaturing agent was revealed by estimating the quantity of the TTR tetramer (first method) or TTR monomer (second method).

2.9 Fibrillogenesis inhibition assay

Evaluation of fibrillogenesis inhibition, due to the protection by ligands, at moderately acidic pH was performed by monitoring the fibrillogenesis kinetics, following the absorbance changes at 400nm. Wt hTTR at 7.2μM was preincubated with 1 or 2 molar equivalents of CSP-1103, Tafamidis, Diflunisal or Flurbiprofen (dissolved in DMSO) at neutral pH (10mM NaP, 100 mM KCl, 1 mM EDTA, pH 7.4) for 3 hour at room temperature, prior to the incubation at acidic pH. The acidic pH was obtained by the addition of an equal volume of 100mM NaAc, 100mM KCl, 1mM EDTA, pH 4.2 (final pH 4.3), at 37° C to promote fibrillogenesis.

2.10 Absorbance estimate of protein concentration

To determine the concentrations of purified RBP and TTR mutant forms, their respective molar extinction coefficient at 280nm were calculated on the basis of their amino acid sequences (Protein Parameters Tool on ExPASy Bioinformatics Resource Portal http://web.expasy.org/protparam).

2.11 RBP-Retinol complex stability

The stability of the RBP-retinol complex was performed in 50mM NaP, 150mM NaCl, pH 7.4 , at 25°C using 10μM holo-hRBP wt, A55T and A57, by recording the decay over time of absorbance intensity in absorption spectrum from 250 to 400 nm.

2.12 Fluorescence spectroscopy

2.12.1 Resveratrol Binding assays

Resveratrol binding assays were performed in 50mM NaP, 150mM NaCl, pH 7.4 , at 25°C. To 2µM proteins (wt hTTR or *Danio rerio* HIUase or hTTR A19I/T119Y) 1 molar equivalent of resveratrol (dissolved in ethanol) was added. Emission spectrum (λ excitation at 320nm) were recorded using an LS-50B spectrofluorometer (Perkin Elmer).

2.12.2 Competitive Resveratrol Binding assays

Fluorescence titrations were performed in 50mM NaP, 150mM NaCl, pH 7.4 , at 25°C. To 2 µM TTR preincubated with 2 µM resveratrol, increasing concentrations of CSP-1103 (λ excitation at 320nm), Tafamidis and Diflunisal were added. Experiments were conducted in triplicate and the IC50 values were calculated as ligand concentrations able to reduce the signal of TTR-bound resveratrol by 50%. Due to the intrinsic fluorescence of uncomplexed Tafamidis and Diflunisal at 390nm (λ excitation at 340nm), fluorescence values were corrected by subtracting the contribution of free ligand for each concentration.

2.12.3 Stabilization of retinol-RBP complexes in the presence of urea

The stability of the wt holo-RBP (2µM), holo-RBP A55T (2µM), holo-RBP A57T (2µM) in the presence or in the absence of 8M urea was evaluated by monitoring the release of retinol, as revealed by the decrease of fluorescence at 460nm (λ excitation at 330nm). Conditions: 50mM NaP, 150mM NaCl, pH7.4, at 25°C.

2.12.4 Fluorescence anisotropy

TTR-RBP interaction was evaluated by means of fluorescence anisotropy analysis. This technique is based on the variation of light polarization emitted by a fluorophore, which in our case is retinol bound to RBP. When a fluorophore is excited by a polarized light, the emission is also polarized and the degree of polarization of emitted light is strictly related to the degree of mobility of the fluorophore. If the fluorophore is able to freely rotate in the medium the resulting anisotropy will be low. A decrease in fluorophore mobility, reflected by TTR-holoRBP complex formation, whose molecular mass is remarkably higher than that of uncomplexed holo-RBP, give rise to a higher anisotropy values. Fluorescent anisotropy measurements, were carried out with 0,5µM holo-hRBP

(wt, A55T and A57T), in 50mM NaP, 150mM NaCl, pH 7.4, at 20°C, by using LS-50B spectrofluorometer (Perkin Elmer) equipped with the accessory for fluorescence anisotropy measurements. Fluorescent anisotropy (A) was determined according to the following equation (1):

$$A = \frac{(I_{\shortparallel} - G * I_{\perp})}{(I_{\shortparallel} + G * I_{\perp})}$$

where $I_{\shortparallel}$ and $I_{\perp}$ are the components of the fluorescence of RBP-bound retinol (excitation at 330nm and emission at 460nm) recorded at an angle of 90°C to the vertically polarized excitation beam and G that is equal to $I_{\perp}'/I_{\shortparallel}'$ (the primes indicating excitation polarized in a perpendicular direction), is the correction for the unequal transmission of differently polarized light. Holo-RBPs were titrated with increasing concentration of hTTR and the increase of fluorescent anisotropy of RBP-bound retinol upon interaction with TTR was monitored. Binding assay was performed in triplicate. The evaluation of the binding parameters was performed using the following equations (2):

$$\alpha^2[RBP]_0 - \alpha(n[TTR]_0 + [RBP]_0 + K_d) + n[TTR]_0 = 0$$

where n is the number of RBP-binding sites, $[RBP]_0$ and $[TTR]_0$ are total molar concentration of RBP and TTR respectively and $\alpha(n[TTR]_0 + [RBP]_0 + K_d)$ is the fraction of RBP bound by TTR (Folli et al. 2005). The value of α was calculated for every point of the titration curve using the following equation (3):

$$\alpha = \frac{(A - A_0)}{(A_{max} - A_0)}$$

where A represents the fluorescence anisotropy value of RBP-bound retinol for a certain molar concentration of TTR, and A_{max} and A_0 are the two limiting anisotropy values, i.e. in the presence of an excess saturating TTR and in the absence of TTR, respectively. The non-linear fit of the equation (2) to the experimentally determined values of A led to the best fitting estimates of binding parameters. The non-linear regression analysis of binding data has been performed using Sigma Plot (Systat Software Inc).

2.13 Crystallization conditions

Both RBP and TTR crystals were prepared by using the vapour diffusion method. To obtain crystal of mutated TTR, hanging drops containing protein at a concentration of 7mg/ml were equilibrated against 50mM NaP, 2M ammonium sulfate, 100mM KCl, pH 7.0 at 25°C. To obtain crystal of mutated holo-RBP, hanging drops containing protein at the concentration of 10mg/ml were equilibrated against 20mM sodium cacodylate, 4.5M NaCl, pH 6.8 at 25°C.

RESULTS AND DISCUSSION

An *in vitro* comparative analysis of the anti-amyloidogenic potential of synthetic inhibitors of transthyretin fibrillogenesis

3.1 Aim of the research

Amyloidosis are particularly relevant human diseases, characterized by the extracellular deposition of normally soluble proteins (Ankarcrona et al. 2016; Sekijima 2015). A large number of synthetic ligands have been tested for their ability to stabilize the native state of TTR, inhibiting fibrillogenesis. Among them, Tafamidis, and Diflunisal (a nonsteroidal antiinflammatory drug - NSAID) were found to be effective in slowing impairment in TTR amyloidosis(Sekijima, Dendle, & Kelly, 2006; Bulawa et al., 2012; Coelho et al., 2012; Berk et al., 2013;). Recently, evidence has been presented to indicate that CSP-1103 (formerly, CHF5074), a derivative of the NSAID Flurbiprofen, protects the native state of TTR according to two distinct lines of evidence (Zanotti et al. 2013; Mu et al. 2015). In this first part a comparative analysis of the interactions of Tafamidis, Diflunisal, CSP-1103 and Flurbiprofen with human wt TTR and of their protective role on the TTR native structure are reported. Considering the ability of CSP-1103 to cross the blood-brain barrier, which is not possessed by Tafamidis and Diflunisal, this could make it a promising candidate for the treatment of leptomeningeal amyloidosis. Consequently the evaluation of the native state stabilization has been extended to the TTR variant A25T, which is associated with this particular type of amyloidosis.

3.2 Expression and purification of wt hTTR

The antyamiloidogenic potential and the affinity for TTR binding sites of CSP-1103, compared to that of Tafamidis and Diflunisal, was initially evaluated for recombinant human wt transthyretin (wt hTTR). In order to perform these kind of studies it is necessary to obtain a high level expression of recombinant protein. The expression of wt hTTR was performed using BL21-CodonPlus strain specifically transformed with the expression vector pET11b containing the wt hTTR gene, taking advantage of the T7 expression system. The induction of the recombinant protein and the solubility after sonication was evaluated by SDS-PAGE, in which it is possible to identify an intense band, corresponding to the molecular weight marker (hTTR wt), missing in the non-induced sample and present in the soluble fraction (**Figure 17**),

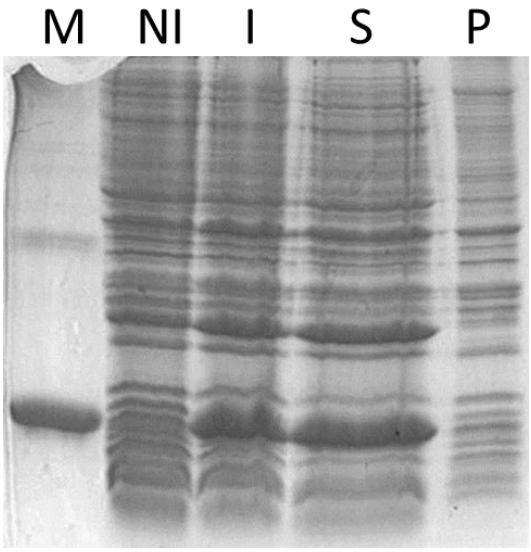

Figure 17. SDS-PAGE showing the induction and the solubility after cell lysis; **M**=wt hTTR marker, **NI**=non-induced cell culture, **I**=IPTG induced cell culture, **S**=supernatant after cell lysis, **P**=insoluble fraction after cell lysis

Purification of wt hTTR was performed by three chromatographic steps, the first of which was an anion exchange chromatography. The choice of this kind of chromatography was based on the ability of the negatively charged Macro-Prep High Q support matrix, to strongly interact with nucleic acids allowing their removal in the first purification step. The concentrated protein sample was applied to the chromatographic column, equilibrated at low ionic strength. Elution was performed using a linear NaCl gradient from 0M to 0.5M and the spectrum of each chromatographic fraction was recorder by spectrophotometric analysis. The fractions with significant absorbance values at 280nm were subjected to SDS-PAGE (15% acrylamide) (**Figure 18**).

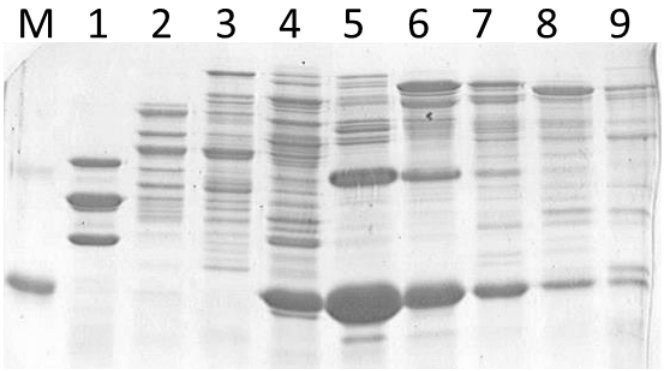

Figure 18. Result of the anion exchange chromatography; lanes **1** to **9** correspond to an elution range from ~ 35% to ~ 85%; **M**=wt hTTR marker

Lanes 4, 5 and 6 (elution at ~70% of the gradient) show an intense band corresponding to the molecular weight of the marker. The fractions in this elution range were combined and concentrated to proceed through the next purification step, a size exclusion chromatography (Ultrogel AcA 54). The fractions with significant absorbance values at 280nm were subjected to SDS-PAGE (**Figure 19**).

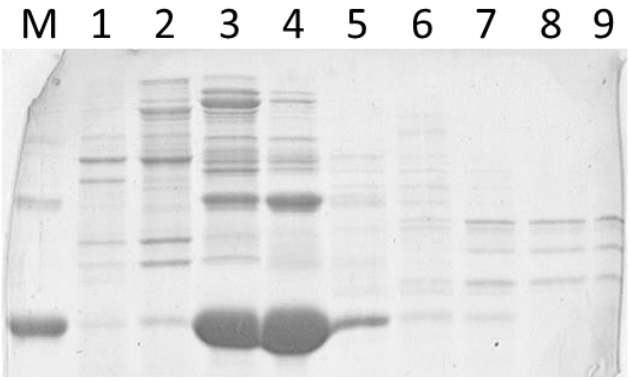

Figure 19. Result of the size exclusion chroamtography; **M**=wt hTTR marker

Lanes 3 and 4 show an intense band corresponding to the molecular weight of the TTR marker. Fraction in this elution range were collected, concentrated and subjected to a hydrophobic interaction chromatography (Phenyl Sepharose 6 Fast Flow) The matrix was equilibrated in Tris HCl 30mM, ammonium sulfate 0.8M, pH7.5 in order to promote hydrophobic contacts. Elution was performed using a linear ammonium sulfate gradient from 0.8 M to 0M. The fractions with significant absorbance values at 280nm were analyzed by means of SDS-PAGE (15% acrylamide) (**Figure 20**). In the gel, always with the main band it is observable a second abundant band with an higher molecular weight. This minor band (**Figure 20**, box) it is actually TTR (perhaps dimeric TTR)

as evaluated by western blotting (data not shown). Fractions from lanes 1 to lane 7 was concentrated and quantified, using the specific extinction coefficient (ε).

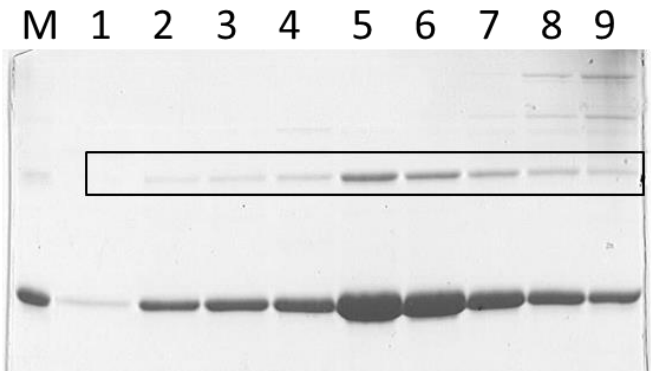

Figure 20. Result of the hydrophobic interaction chromatography ; **M**=wt hTTR marker

3.3 Competitive binding assay to recombinant hTTR

Initially fluorescence measurements were carried out to study the affinity of CSP-1103, Tafamidis and Diflunisal for the TTR binding sites. This interaction was evaluated by competitive binding experiments with resveratrol, a fluorescent ligand able to specifically interact with the TTR binding site. The fluorescence emission of resveratrol, which is nearly negligible for the unbound compound in solution, increases substantially upon binding to TTR, so that it could be exploited to evaluate the binding of possible competitors. Due to the lack of fluorescence of CSP-1103, titrations were carried out by using λ excitation at 320nm reading the emission fluorescence at 390nm (λ_{max}), to monitor the displacement of TTR-bound resveratrol, while for Tafamidis and Diflunisal, to avoid interference with their fluorescence properties, similar competitive binding experiments were conducted by using λ excitation at 340 nm. TTR preincubated with resveratrol was titrated by using increasing concentrations of each competiror. In these condition, the addition of Tafamidis and CSP-1103 (**Figure 21**, green and orange dots) led to a significat decrease of resveratrol fluorescent signal (**Figure 21**, blue dots). Titrations were perfomed in triplicate and allowed us to calculate the IC50 values (ligand concentrations able to reduce the signal of TTR-bound resveratrol by 50%). Very similar IC50 values for CSP-1103 and Tafamidis were estimated showing high affinity for TTR, and a lower affinity for Diflunisal was evaluated (**Figure 21**).

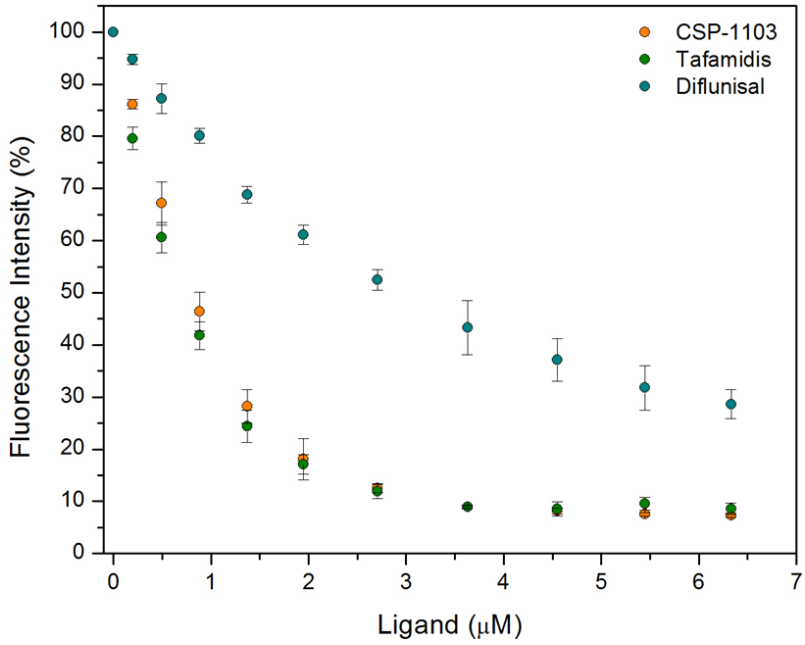

Drug	IC50 (μM)
CSP-1103	0.75
Tafamidis	0.63
Diflunisal	1.91

Figure 21. Competitive fluorescence titrations

3.4 Stabilization of recombinant hTTR – urea denaturation

To compare the stabilizing effect of CSP-1103, Tafamidis, Diflunisal and Flurbiprofen on wt hTTR , the ability of this molecules to inhibit the TTR tetramer denaturation in the presence of high concentration of urea was studied. Urea enhances the tetramer to monomer transition, which is believed to be the rate limiting step for amyloid fibril formation (Colon and Kelly 1992; Lai, Colón, and Kelly 1996). The relative amount of tetramer and monomer species can be evaluated and quantified after cross-linking with glutaraldehyde, a bifunctional molecule used as fixative, followed by SDS-PAGE. Crosslinking between subunits permit to discriminate, after SDS-PAGE, bands corresponding to the three different oligomeric states of TTR (tetramer, dimer and monomer). **Figure 22** shows a reference image of SDS-PAGE where oligomeric states of TTR are marked and an histogram, reporting the relative amounts of monomer after urea denaturation. The addition of CSP-1103, Tafamidis and Diflunisal has a significant stabilizing effect, with a monomer reduction of at least 50%. Instead, Flurbiprofen possesses only a weak stabilizing effect (**Figure 22**).

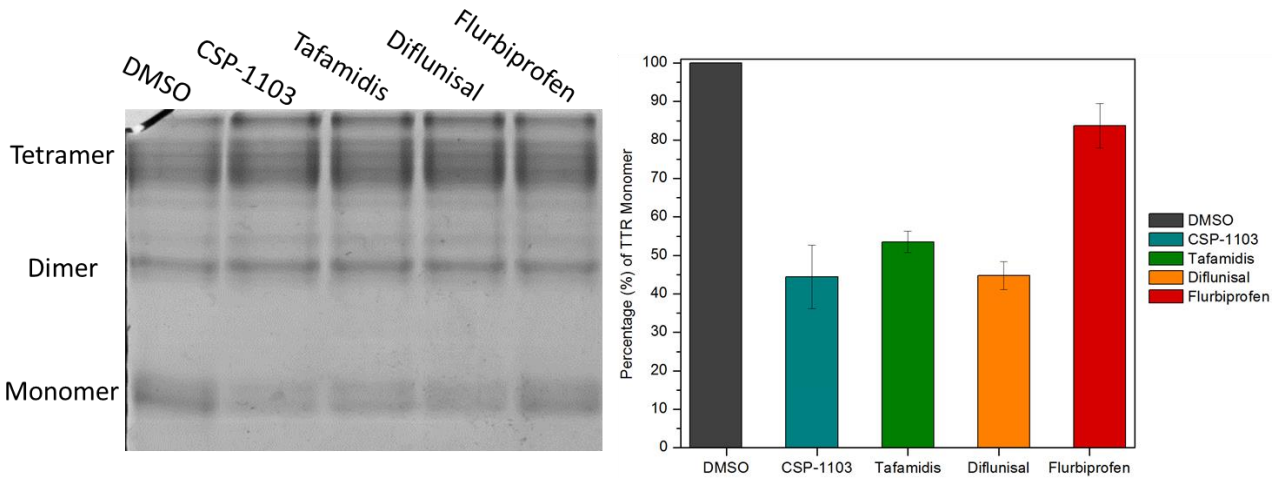

Figure 22. Representative SDS-PAGE after urea denaturation and histogram representing relative monomer quantities

3.5 Stabilization of recombinant hTTR – acidic denaturation

Considering that fibril formation seems to be induced by a moderately acidic pH, as demonstrated by Kelly and co-worker (Colon and Kelly 1992; Lai, Colón, and Kelly 1996), the stabilization of the native state of TTR and consequently the inhibition of aggregation at moderately acidic pH (4.3) was analyzed. After incubation of wt hTTR with CSP-1103, Tafamidis, Diflunisal or Flurbiprofen, the increase in turbidity estimated as absorbance signal at 400nm was monitored over time. **Figure 23** shows precipitation kinetics for wt hTTR in the presence of 1 molar equivalent (left) or 2 molar equivalents (right) of the tested compounds. Tested compounds slow down the precipitation kinetics and decrease the absorbance at 400nm at the end of the incubation. The results of both experiments indicate a strong stabilizing effect for CSP-1103, Tafamidis and Diflunisal relative to the DMSO control. Flurbiprofen prevents aggregation, only to a minor extent (**Figure 23**, red dots). In the presence of 2 molar equivalents, the stabilizing effects of CSP-1103, Tafamidis and Diflunisal are similar, and it is not possible to identify differences between them. Data obtained for the experiment at 1 molar equivalent reveal the greatest stabilizing effect by Tafamids, the weakest effect by Diflunisal and an intermediate stabilizing effect by CSP-1103.

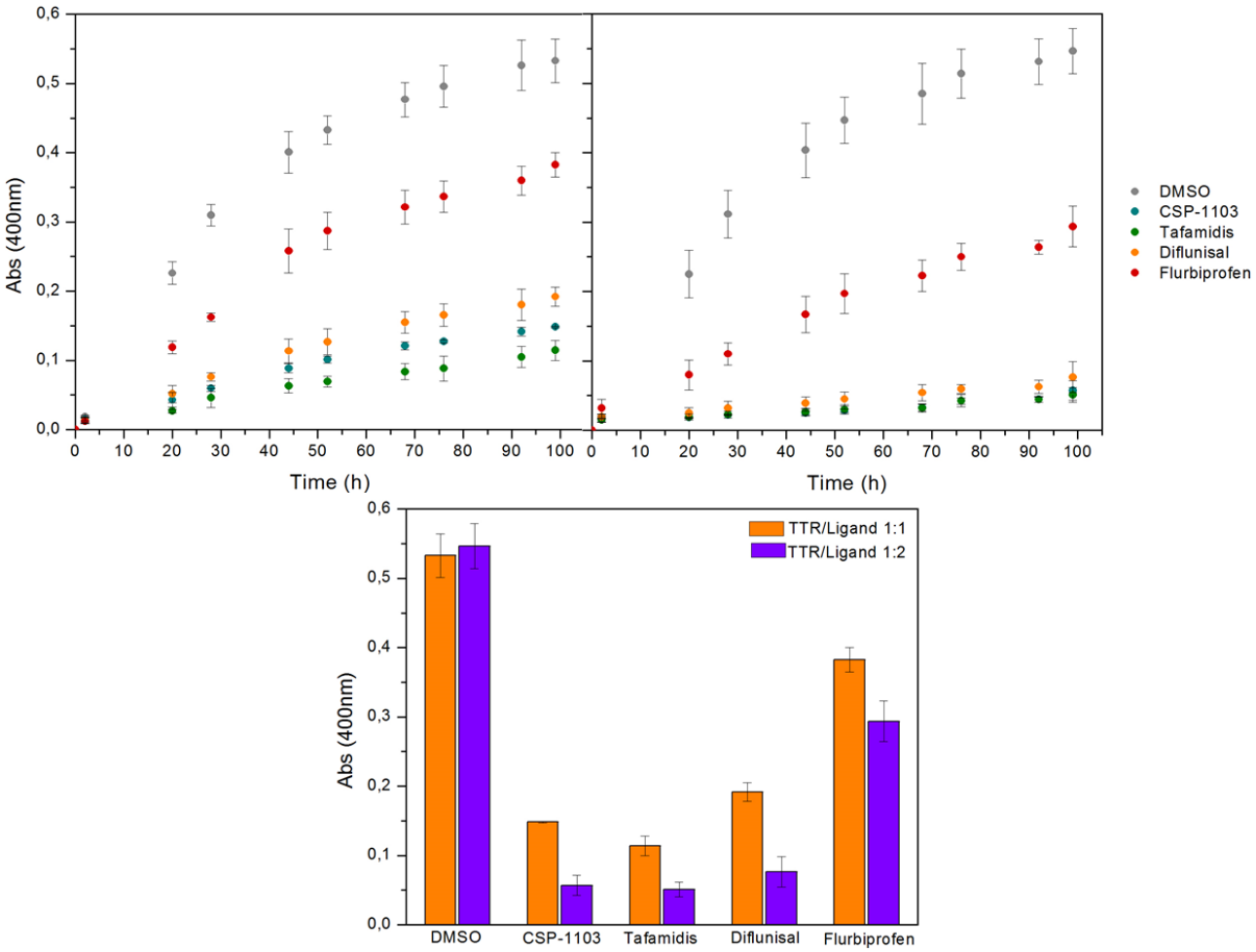

Figure 23. Precipitation kinetics with 1 molar equivalent of tested compounds (left) and 2 molar equivalent of tested compounds (right); the histogram show maximum absorbance at 400nm after 99h for tested compounds

3.6 Stabilization of plasma hTTR

Previous experiments on recombinant transthyretin showed the ability of CSP-1103 not only to interact with TTR binding site, with high affinity, but also to stabilize the TTR native state preventing unfolding and consequently aggregation. At this point a key issue to be addressed is the ability of CSP-1103 to interact and to stabilize TTR in a more complex environment, resembling *in vivo* condition. *Ex vivo* urea denaturation experiments were therefore carried out using human plasma, obtained from healthy donor, in order to evaluate native state stabilizing effect on plasma wt TTR .

First Method:

Initially, the experiments were carried out with CSP-1103, Tafamidis, Diflunisal and Flurbiprofen at a unique concentration of 30μM. The method is the same as that of with recombinant TTR, but plasma samples were subjected to crosslinking at two stages: just after urea addition (Time=0h) and after 24h incubation with 6M urea (Time=24h) at 4°C. Considering the high protein concentration present in human plasma, the evaluation of the native state stabilization, requires as a further step Western Blotting. **Figure 24** shows a representative SDS-PAGE, where the corresponding position of TTR oligomeric states are shown, along with an enlarged view of crosslinked tetramer.

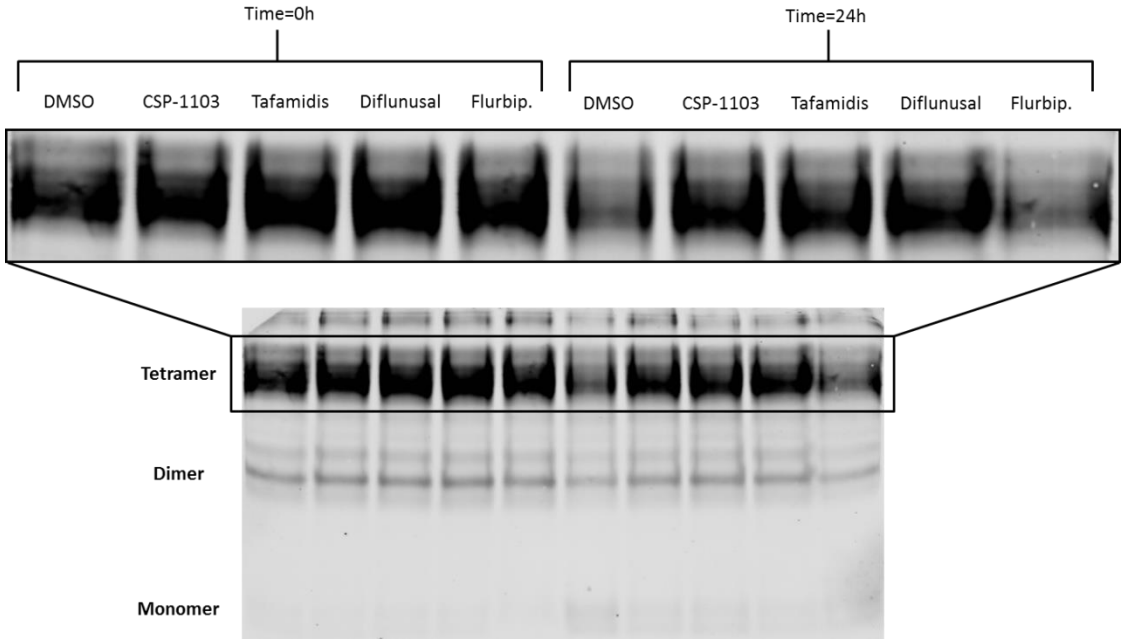

Figure 24. Representative SDS-PAGE after urea denaturation of plasma transthyretin and enlarged view of TTR tetramers

It is possible to evaluate the stabilizing effect of each ligand by considering the intensity of the tetramer TTR bands after 24h incubation, relative to time 0h and DMSO control. Only the presence of CSP-1103, Tafamidis and Diflunisal determine a good, but very similar, stabilizing effect. This results is in good agreement with those previously observed for recombinant TTR in the presence of urea. To better compare the stabilizing effect of the three effective molecules, the same experiment was performed using lower ligand concentrations (7.5, 15 and 30μM) (**Figure 25**).

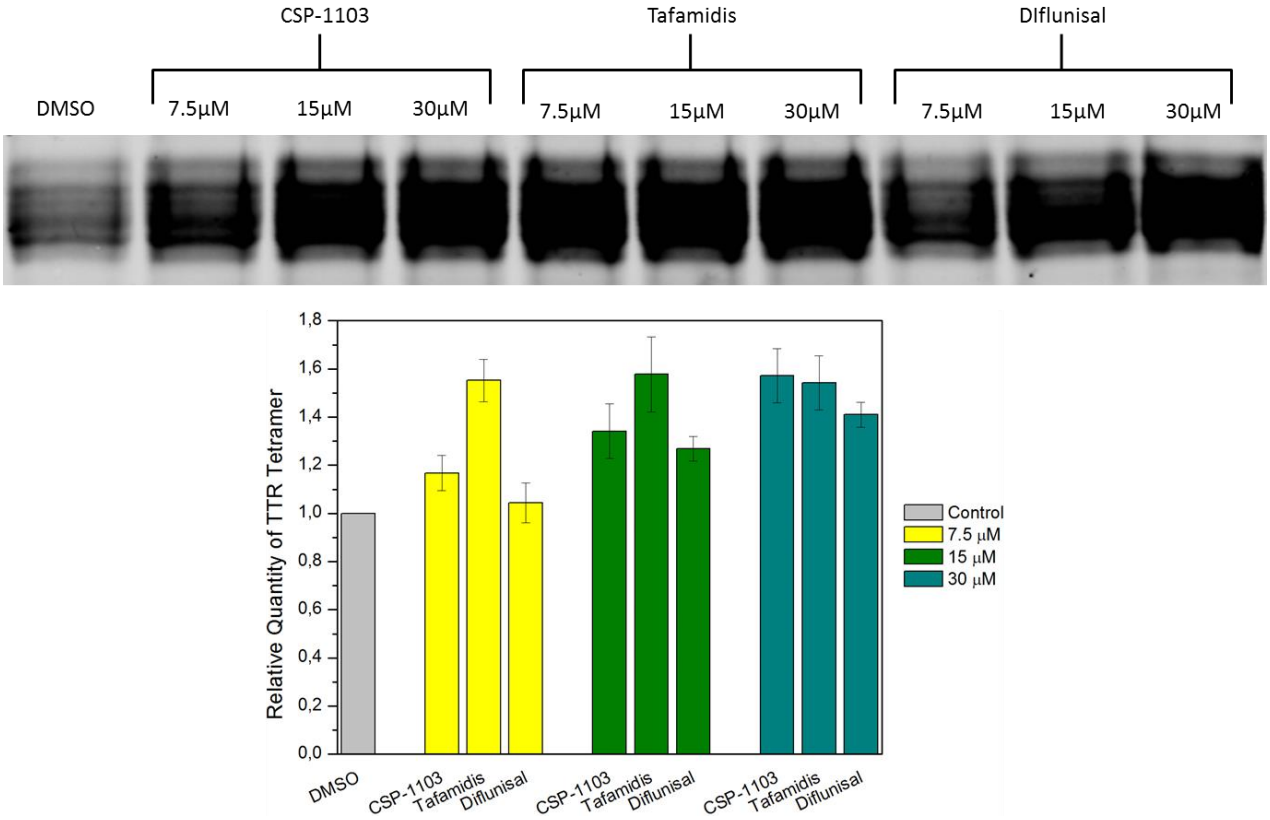

Figure 25. Enlarged view of TTR tetramer and histogram representing the relative quantity of tetramer for each conditions, compared to DMSO control

Tafamidis appears to be the most effective ligand in particular at the lowest concentration of 7.5µM. The stabilizing effects of CSP-1103 and Diflunisal appear to be very similar in all conditions.

Second Method:

In order to further discriminate the stabilizing effect of CSP-1103 and Diflunisal a second distinct method was used, in which mild denaturation conditions prevent re-association of TTR monomer but do not denature TTR tetramer (Nilsson et al. 2016). In particular, this method allow us to estimate the stabilizing effect of the ligand by evaluation of the quantity of monomer after incubation of plasma samples treated with TTR ligands with 4M urea for 18h, at 20°C. After this step, protein samples are analyzed by SDS-PAGE, in the presence of a low SDS concentration (0.86mM). Finally, Western Blotting is performed to monitor the aggregation state of TTR in plasma samples. The results (**Figure 26**) show again the greatest stabilizing effect of Tafamids relative to CSP-1103 and DIflunisal. As found in the previous experiment the stabilizing effect by CSP -1103 and Dilfunisal is very similar.

Our data demonstrate that CSP-1103 is able to interact with TTR in a complex environment like human plasma, stabilizing the native state of TTR to an extent similar to that of Diflunisal.

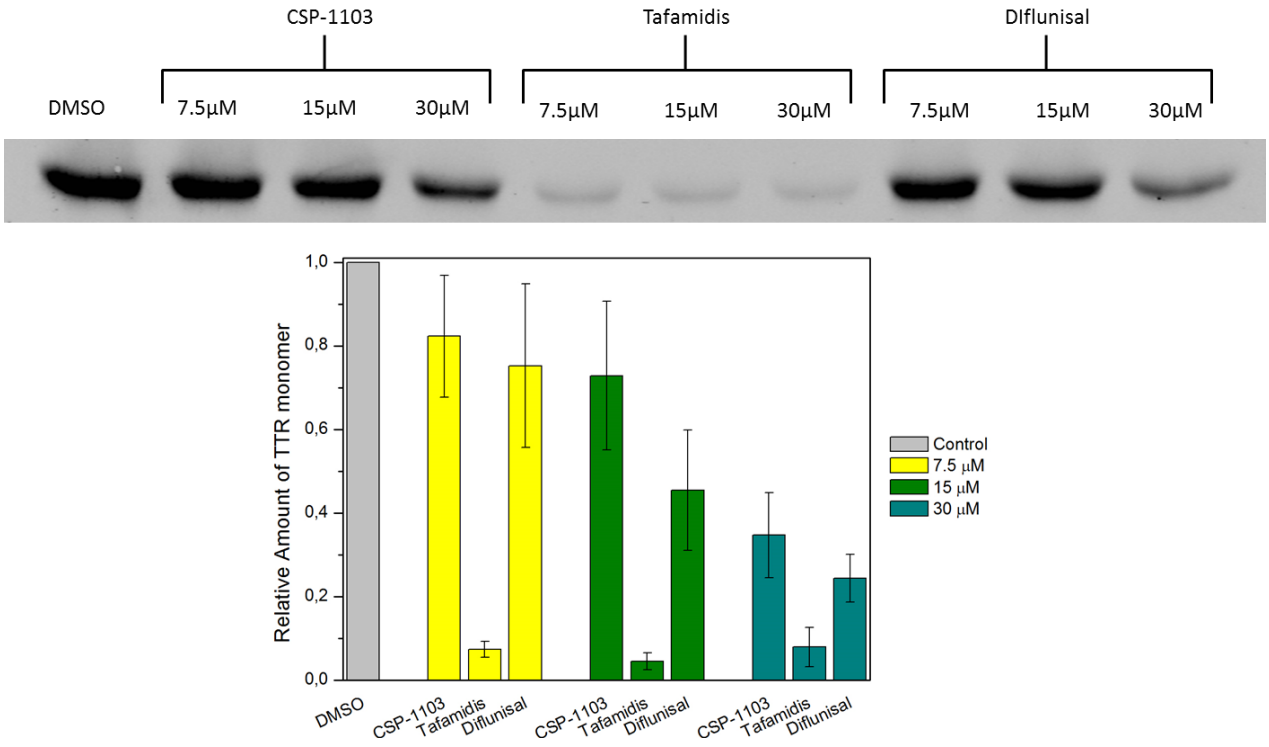

Figure 26. Enlarged view of TTR monomers and histogram representing the relative quantity of monomer for each conditions, compared to DMSO control

3.7 Expression and purification of hTTR A25T

Considering the ability of CSP-1103 to cross the blood-brain barrier (Mu et al. 2015), the stabilizing effect was also evaluated using one of the different mutant forms associated with leptomeningeal amyloidosis, hTTR A25T. For the expression and purification of this mutant form the same conditions as for wt hTTR could be adopted (data not shown).

3.8 Stabilization of recombinant hTTR A25T

In order to compare the stabilizing effect of CSP-1103, Tafamids, Diflunisal and Flurbiprofen on transthyretin A25T, urea denaturation experiment were performed. Results (**Figure 27**) show a better stabilizing effect for Tafamids and CSP-1103 which determine a reduction of monomer of approximatively 80% and 60% respectively. However it is important to consider that Tafamidis (as Diflunisal) is not able to cross the blood-brain barrier, so that despite its greater stabilizing effect, such effort cannot be exploited *in vivo*. Diflunisal result to be the weakest TTR stabilizer.

It is interesting to note that CSP-1103 possesses a greater stabilizing effect on this mutant form relative to wt hTTR.

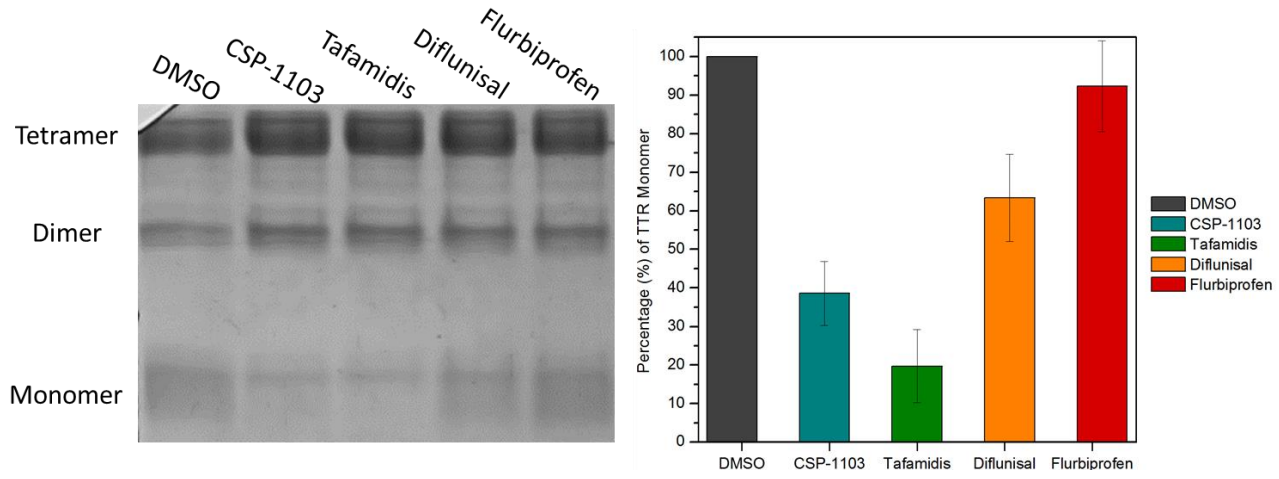

Figure 27. Representative SDS-PAGE after urea denaturation and histogram representing relative monomer quantities

3.9 Discussion

Amyloidoses represent a group of degenerative diseases caused by protein misfolding and misassembly leading to fibril accumulation in tissues. Among proteins associated with such pathologies we also find transthyretin. Tafamidis and Diflunisal, two synthetic organic molecules, have shown their effectiveness in clinical trials. Tafamidis, approved in Europe and Japan for the treatment of FAP diseases, possesses high affinity for the TTR binding sites, a strong stabilizing effect and is able to slow the progression of the disease, but was found to be ineffective in the late stages of the pathology (Bulawa et al. 2012; Coelho et al. 2012). Diflunisal was also found to be effective in the therapy of affected patients and possesses a high oral viability, but has a lower stabilizing effect relative to Tafamidis and produces significant side effects (Sekijima, Dendle, and Kelly 2006; Berk et al. 2013). Furthermore, both Tafamidis and Diflunisal cannot penetrate the blood-brain barrier becoming useless in the rather rare cases of TTR leptomeningeal amyloidosis. The possibility to find new molecules with good ability to inhibit TTR misfolding and aggregation *in vivo*, with high viability and able the enter the central nervous system is thus of great interest. CSP-1103, a molecule derived from the NSAID Flurbiprofen able to penetrate the blood-brain barrier was initially investigated as anti-Alzheimer compound (Imbimbo et al. 2009; Ross et al. 2013), but it has recently been shown its ability to specifically recognize TTR (Zanotti et al. 2013; Mu et al. 2015). This study was conducted in order to evaluate the stabilizing ability of CSP-1103 on TTR tetramer in comparison with Tafamidis and Diflunisal, the two molecules available for therapeutic use, and with its precursor Flurbiprofen. In TTR tetramer stabilization assays conducted in the presence of urea using recombinant wt hTTR, CSP-1103 have shown similar stabilizing effect in comparison with Tafamidis and Diflunisal. Moreover, *ex vivo* experiments have shown the ability of the CSP-1103 to specifically recognize TTR in plasma and to stabilize the TTR tetramer. Although Tafamidis showed the strongest stabilizing effect, both CSP-1103 and Diflunisal proved to be good TTR stabilizer. Denaturation experiments conducted on the TTR mutant A25T showed the ability of CSP-1103 to stabilize the TTR native state greater than that of Diflunisal. Although Tafamidis is a better TTR stabilizer, its inability to cross the blood-barrier prevents its use in leptomeningeal amyloidosis. By considering its capacity to specifically recognize TTR and stabilize the TTR tetramer in plasma , associated to its high life time in blood and its ability to penetrate the blood-brain barrel, CSP-1103 represents a good candidate for the therapy of TTR amyloidosis, especially for leptomeningeal amyloidosis.

Engineering human transthyretin to restore an ancient therapeutically relevant enzymatic activity

4.1 Aim of the research

Protein engineering has been widely used to modify enzyme properties, such as stability under denaturing conditions or substrate specificities. In this study our aim of protein engineering rational approach was to obtain an enzyme suitable for the treatment of hyperuricemia and gout. Humans are not able to degrade uric acid because of the lack of the pathway responsible for its catabolism (Oda et al. 2002; Ramazzina et al. 2006). This condition together with different other factors, determine an increase of uric acid level in plasma, which is responsible for hyperuricemia diseases (Lesch and Nyhan 1964; Graessler et al. 2006; Brandstatter et al. 2008). Different therapeutic strategies have been proposed to counteract hyperuricemia, one of which use a pegilated pig-baboon urate oxidase (Pegloticase), which is able to convert uric acid into the more soluble 5-hydroxyisourate (5-HIU). It is important to note, however, that intermediate products of uric acid degradation seems to be toxic (Santos, Anjos, and Augusto 1999). TTR and HIUase share an almost identical quaternary structure and the only differences are localized in the binding or active site, respectively (Zanotti et al. 2006; Cendron et al. 2011). Therefore, human transthyretin binding sites were redesigned, by site-directed mutagenesis, introducing in the T4 binding cavities catalytic residues present in an authentic HIUase, to restore the ancestral hydrolase activity, lost during evolution. This engineered TTR could be used, together with Pegloticase, in order to speed up uric acid degradation and to decrease toxicity of intermediate products. Last but not least, an important feature of this mutated TTR, would be the presumably lack of immunogenicity of the human TTR scaffold, which would prevent the deleterious immune reactions induced by the administration of therapeutic agents, of non-human HIUases.

4.2 Identification of residue replacements

Initially it was necessary to identify the key catalytic residues present in the active site of hidroxyisourate hydrolase (HIUase), involved in the conversion of the substrate 5-hydroxyisourate (5-HIU) to 2-oxo-4-hydroxy-4-carboxy-5-ureidoimidazoline (OHCU). In this regard the residues replacements were chosen based on the results of previous studies conducted on four HIUases from different organisms: *Danio rerio*, *Salmonella Dublin*, *Bacillus subtilis* and *Klebsiella pneumoniae*. Regarding *Danio rerio* HIUase, Cendron et al. (2011) have previously shown that a small number of critical mutations, affecting the enzyme active site are sufficient to generate a drastically different function, leading to the open up of the cavity, thereby allowing binding of T4. For the other three HIUases, different mutagenic studies have been performed in order to clarify the mechanism of action and to identify the main catalytic residues (Hennebry et al. 2006; Jung et al. 2006; French and Ealick 2011) . Based on all these information, five residue replacements were chosen.

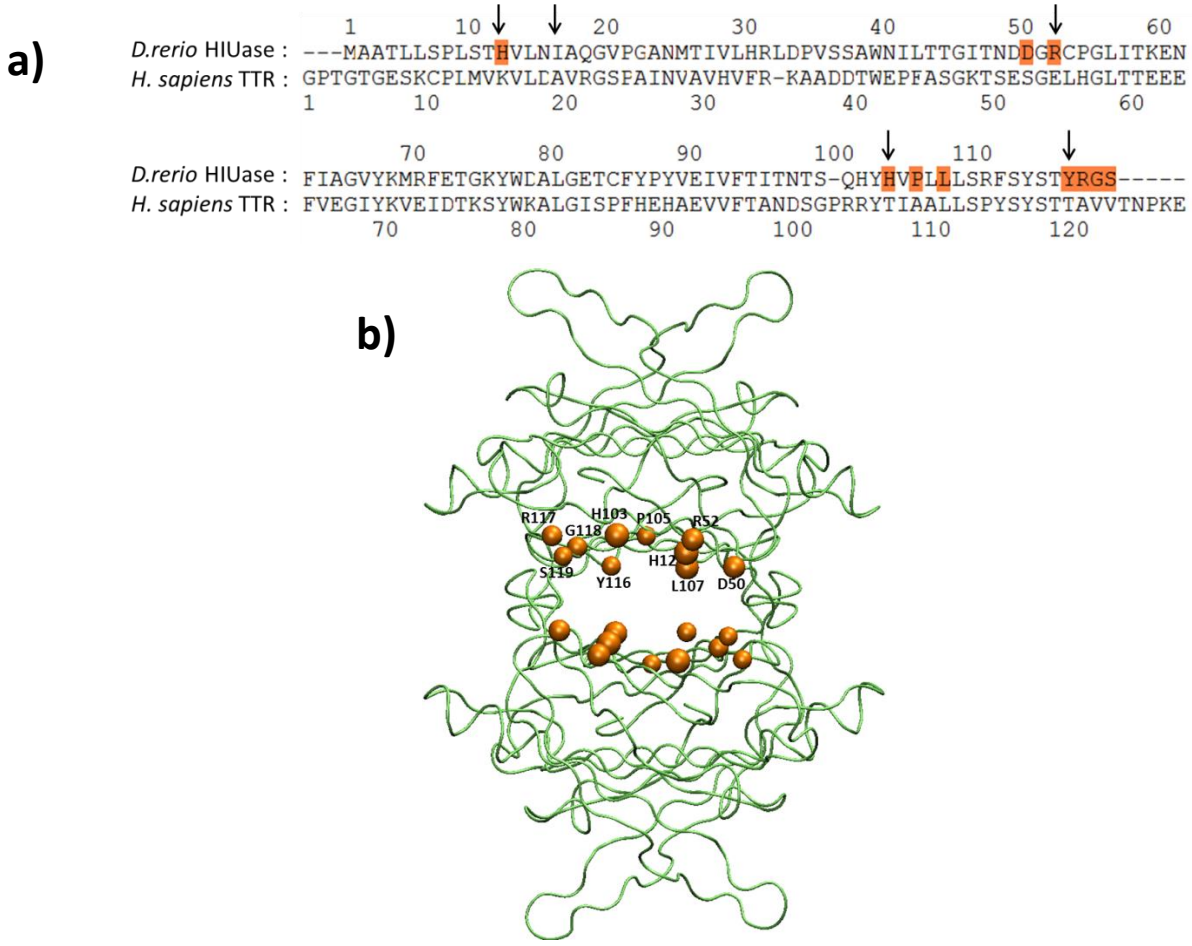

Figure 28.a) Amino acid sequence alignment of human TTR and *Danio rerio* HIUase. The alignment was constructed with MEGA4 (Tamura et al. 2007) and rendered with GeneDoc (Nicholas and Nicholas 1997); b) Cα chain trace of *Danio rerio* HIUase (PDB ID: 2H1X), conserved residues are in orange. The structure representation was obtained by using Visual Molecular Dynamics (VMD) (Humphrey, Dalke, and Schulten 1996). This figure was adapted from (Zanotti et al. 2006)

Figure 28.a shows a sequence alignment of a representative HIUase (*Danio rerio*) and human TTR in which residues participating in the formation of the active site, which are conserved in all HIUases, are shaded in orange in the *Danio rerio* HIUase sequence, while residues mutated to restore hydrolase activity are indicated with arrows. In **Figure 28.b** the position of the conserved residues are marked in orange in the *Danio rerio* Hiuase cavity.

4.3 Site-directed mutagenesis, expression and purification of TTR mutant forms

Quick change site-directed mutagenesis was used to obtain all TTR mutant forms, indicated:

- hTTR A19I/T119Y → TTR MUT2
- hTTR A19I/E54R/T119Y → TTR MUT3
- hTTR K15H/A19I/E54R/T119Y → TTR MUT4.1
- hTTR A19I/E54R/T106H/T119Y → TTR MUT4.2
- hTTR K15H/A19I/E54R/T106H/T119Y → TTR MUT5

All mutations were inserted one by one, in order to evaluate the functional and structural properties of each mutant form, as described below. For the expression and purification of this mutant form the same conditions as for wt hTTR (Materials and Methods 2.5 and 2.6 section) could be adopted (data not shown).

4.4 TTR binding site narrowing - A19I and T119Y replacements

The first step aimed to modify the inner volume of the TTR binding sites by insertion of residues able to narrow the cavity, making it similar to that of HIUase. With the substitution of the human TTR residues Ala19 and Thr119 with the corresponding residues present in the *Danio rerio* HIUase, we obtained the first double mutant hTTR MUT2. Evaluation of the narrowing of the cavity was performed by using resveratrol binding assay. Resveratrol is a probe whose fluorescence is induced by the interaction with the TTR binding sites. Upon addition of resveratrol to wt hTTR, TTR MUT2 and *Danio rerio* HIUase, only wt hTTR showed a fluorescent emission signal (**Figure 29**), indicating the reduction of the size of the cavity. Furthermore, the TTR MUT2 form was crystallized and structural data was obtained in collaboration with Professor Giuseppe Zanotti (University of Padua). In **Figure 30**, in which structural details of the changes present in the binding site of TTR upon mutation are shown, one of the two replacements, T119Y leads to the major occupancy and narrowing of the cavity at the bottom of the cleft (Orange). The second residue which directly reduces the dimension of the cavity is Leu110 (Green).

Although this is a conserved residue in both HIUases and TTRs, its different position in the two proteins is due to the second substitution A19I (Yellow). This conformational change, after residue replacement, was previously observed by Cendron et al. (2011) for the opposite situation, in the *Danio rerio* HIUase. The second replacement (A19I) is not directly related to the narrowing of the cavity, but it's contribution is indirect. In the image a fourth residue is marked and corresponds to the Lys15 (Purple). As it may appear from the figure, the two lysines point toward the center of the binding site, generating a substantial occupancy. However, it should be noted that in the two binding sites of both wt hTTR and hTTR MUT2 , different positions of the side chain of Lys15 are found.

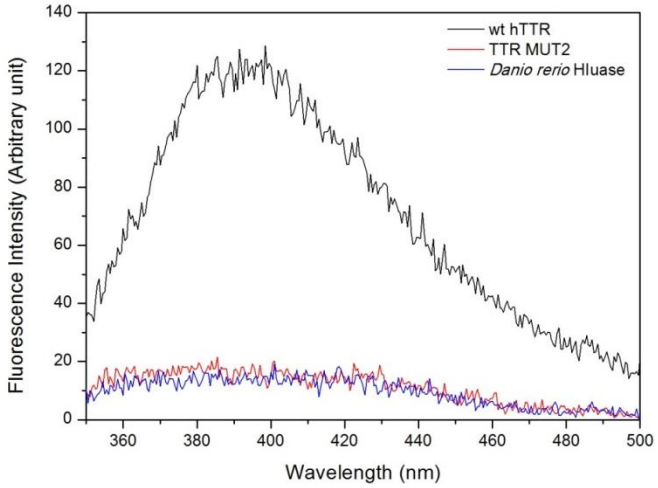

Figure 29. Emission spectra of resveratrol bound to wt hTTR, TTR MUT2 and *Danio rerio* HIUase

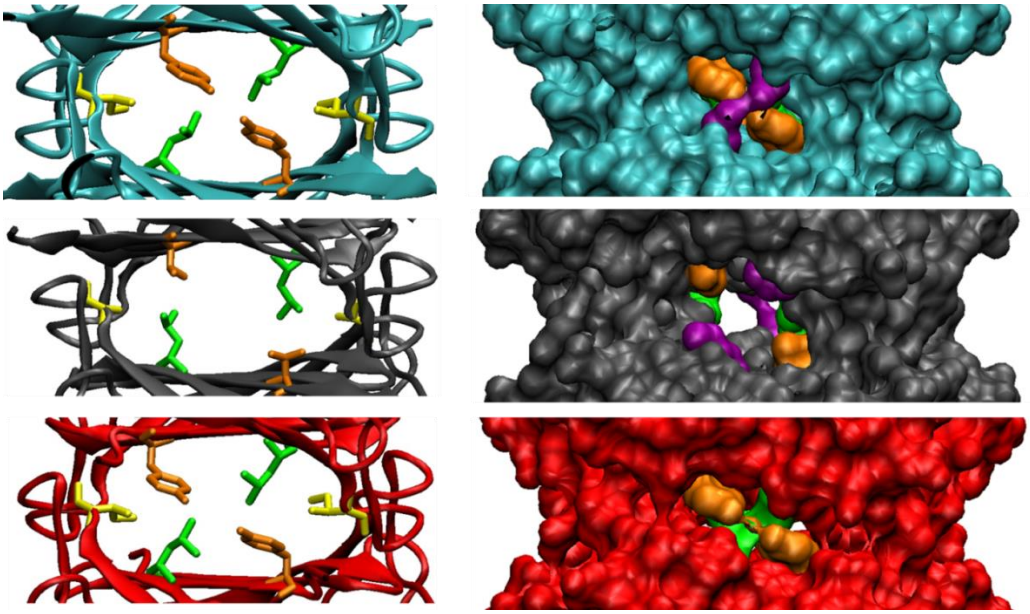

Figure 30. Comparison of structural details present in the cavities of TTR MUT2 (cyan), wt hTTR (Grey) (PDB ID:14F1) and *Danio rerio* HIUase (Red) (PDB ID: 2H1X). The structure representations were obtained by using Visual Molecular Dynamics (VMD) (Humphrey, Dalke, and Schulten 1996).

An enzymatic assay conducted with the double mutant TTR MUT2 did not reveal any enzymatic activity. In fact, the same spontaneous decay was determined in the absence and in the presence of the double mutant (**Figure 31**). Overall, A19I and T119Y replacements were able to narrow the T4 binding sites of TTR as demonstrated by fluorescent measurements and structural data analysis. However, no catalytic activity was found for TTR MUT2.

4.5 First Catalytic residue replacement – E54R

At this point the first hypothetical catalytic residue was inserted in the TTR MUT2 form, replacing Glu54, localized at the entrance of the cavity, with an Arg (mutation E54R). This substitution had two aims. The first one was the introduction of a positive charge in the active site, a common features of HIUases, as opposed to the negative charge presents in the TTR binding sites(Hennebry et al. 2006). The second one was the introduction of a residue potentially able to stabilize the oxyanion, which has been proposed to represent a reaction intermediate (French and Ealick 2011). The triple mutant form (TTR MUT3) exhibit a very low enzymatic activity (**Figure 31**).

4.6 Second and Third catalytic residue replacements - K15H and T106H

Subsequently, in the sequence of the TTR MUT3 other two mutations were added to the triple mutant, to obtain two distinct mutant forms (TTR MUT4.1 and TTR MUT4.2). With these substitutions, respectively K15H and T106H, have been introduced two catalytic residues presumably involved in the nucleophile activation in HIUase. Enzymatic assays (**Figure 31**) showed a substantial increase of the rate of 5-HIU degradation for both mutants, with a greater activity for TTR MUT4.2 (T106H substitution). In **Figure 31** an enzymatic kinetic performed with *Danio rerio* HIUase, is also reported at a concentration three order of magnitude lower than that of mutated TTR. This seems to indicate a greater importance, in the active site, for the His replacement in position 106 of that at position 15. This finding is not in agreement with previous mutagenic studies conducted on bacterial HIUases, in which the substitution of the corresponding His15 led to a greater decrease in enzymatic activity (Hennebry et al. 2006; Jung et al. 2006 French and Ealick 2011). In fact, it has been hypothesized that this histidine may be the direct nucleophile activator, able to deprotonate a water molecule. The explanation may lie in the residue that is present at position 15 in TTR MUT4.2 binding sites. Activation of a nucleophile in a catalytic dyad/triad inside an active site, requires a residue which acts as a base in order to polarize and deprotonate the nucleophile. In the TTR MUT4.2 active sites, instead of a His at position 15 is present a Lys. This residue, which is a stronger base, could activate by itself the water molecule

and this may explain the observed result. TTR MUT4.2 shows an enzymatic activity of approximatively 2000 fold lower than *Danio rerio* HIUase. At this point the TTR mutant form containing both main catalytic residues (15H, 106H) was obtained (TTR MUT5). The enzymatic assay (**Figure 31**) unexpectedly showed a loss of activity instead of an increase. We suspected that a mutations overload at the active site would cause a local destabilization of the active site region, with concomitant enzyme inactivation.

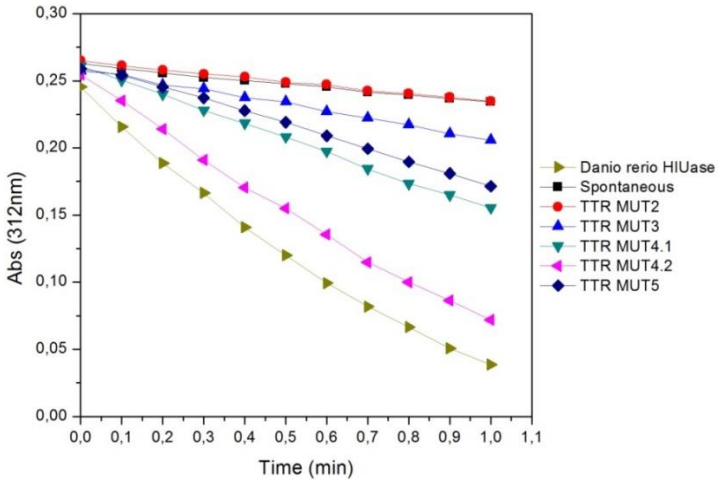

Figure 31. Enzymatic assays

4.7 Interaction of TTR MUT4.2 with human holo-RBP

The best product of site directed mutagenesis we have obtained in terms of recovery of enzymatic activity, (TTR MUT4.2) was further analyzed, to establish whether the ability of this mutant form to interact with RBP, a feature diagnostic of well conserved 3D structure, was maintained. Indeed, the binding curves for the interaction of TTRMU4.2 and wt TTR nearly superimpose (**Figure 32**), consistent with the lack of significant changes in the mutated protein outside the enzyme active site.

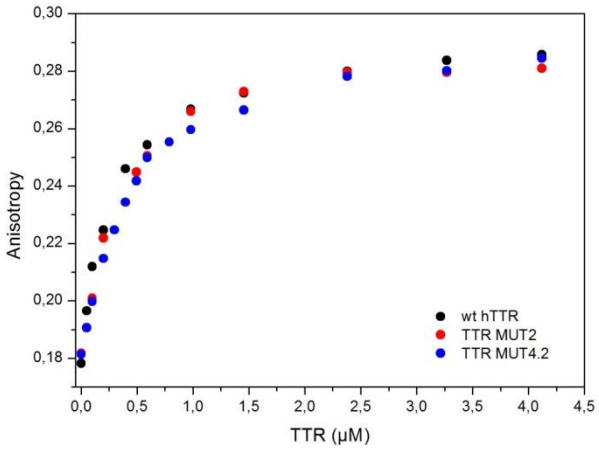

Figure 32. Fluorescent anisotropy titrations for the wt hTTR, hTTR MUT2 and hTTR MUT4.2

4.8 Discussion

Nowadays different proteins are used as therapeutic agents for the treatment of different kinds of diseases and as a viable alternative to the use of drugs consisting of small molecules. A relevant example is provided by the treatment of hyperuricemia and gout in which small molecules or recombinant pegilated urate oxidase are used to slow disease progression (Gliozzi et al. 2016). A major obstacle to the use of proteins as therapeutic agents is their immunogenicity, which may be responsible for deleterious immune reactions in humans. Transthyretin and HIUase, the second enzyme of the uric acid catabolic pathway, are closely related from an evolutionary and structural point of view, sharing a very close quaternary structure (Cendron et al. 2011; Zanotti et al. 2006). Considering all this information hTTR was engineered by site directed mutagenesis to restore the ancient HIUase enzymatic activity, with the final aim to design enzyme active sites within a human protein scaffold possibly devoid of immunogenicity and, therefore, suitable for the treatment of hyperuricemia. The narrowing of the T4 binding site cavities in TTR was achieved by the substitution A19I and T119Y, located at the bottom of the cavities. The introduction of the two mutations in TTR prevented resveratrol binding, indicating a reduction of the size of the cavities, a result supported by X-ray analysis. The maximal activity, it was about 2000 fold lower than that of an authentic HIUase, was achieved with the additional mutations E54R and T106H. This multiple mutant form has maintained its overall original 3D structure, as revealed by its ability to interact very well with RBP, in a manner indistinguishable from that of wt TTR. In conclusion, by engineering human TTR we have obtained an enzymatic HIUase activity, maintaining the protein scaffold of TTR. This study does not only demonstrate the possibility to recover an ancestral enzymatic activity, but also shown how the TTR binding sites could be modified in order to bind an enzymatic substrate very different form the large T4 molecule. hTTR MUT2 is a stable protein which could be used as a starting human scaffold for protein engineering approaches.

Functional analysis of two pathological forms of human Retinol Binding Protein (RBP)

5.1 Aim of the research

Vitamin A deficiencies (VAD) are associated with different types of disorders that affect primarily the visual system (Wilson, Roth, and Warkany 1953; Dowling and Wald 1958; See and Clagett-Dame 2009). These disorders may be caused by the lower intake of vitamin A with the diet or by mutations in different proteins such as RBP (Biesalski et al. 1999; Folli et al. 2005) and STRA6 (Stimulated by Retinoic Acid) (Chassaing et al. 2009; Casey et al. 2011), which is involved in the retinol transport. Recently, Chou et al. (2015) identified two new mutations on the RBP gene associated to an autosomal dominant form of MAC, a pathology characterized by structural eye defects. These two mutations (A55T and A57T) are localized at the bottom of the retinol binding protein cavity in proximity to the retinol β-ionone ring. Chou et al. (2015) have reported that these mutant forms present an impaired retinol binding and hypersensitivity to nonpolar or amphipathic conditions, while the interaction with STRA6 was enhanced. The authors have hypothesized that such enhancement would be associated with a reduced vitamin A delivery, leading to the pathological alterations. In this study we have obtained the two recombinant RBP mutant forms (A55T and A57T) in order to further clarify their pathological role and to obtain structural data, through the analysis of their functional and structural properties.

5.2 Expression and purification of wt and mutant forms of hRBP

The expression of both wt and mutant forms of hRBP , that required an unfolding/refolding step was performed essentially as described (Material and Methods 2.5.2), followed by protein purification (Material and methods 2.6 section) (data not shown).

The absorption spectrum of the recombinant holo-RBP shows the characteristic absorbance peak with a maximum at 330nm, in addition to that at 280nm, due to RBP-bound retinol. Ideally a completely saturated holo-RBP should present a ratio of the absorbances at 280nm and 330nm equal or close to 1. Upon heterologous expression and purification, wt hRBP, A55T and A57T exhibited different absorption spectra(**Figure 33**). In particular wt hRBP and A57T presented the characteristic absorbance at 330nm and a 280:330 nm ratio of approximatively 0.84 and 0.5 respectively, while hRBP A55T did not show any absorbance at 330nm, indicating the absence of bound retinol.

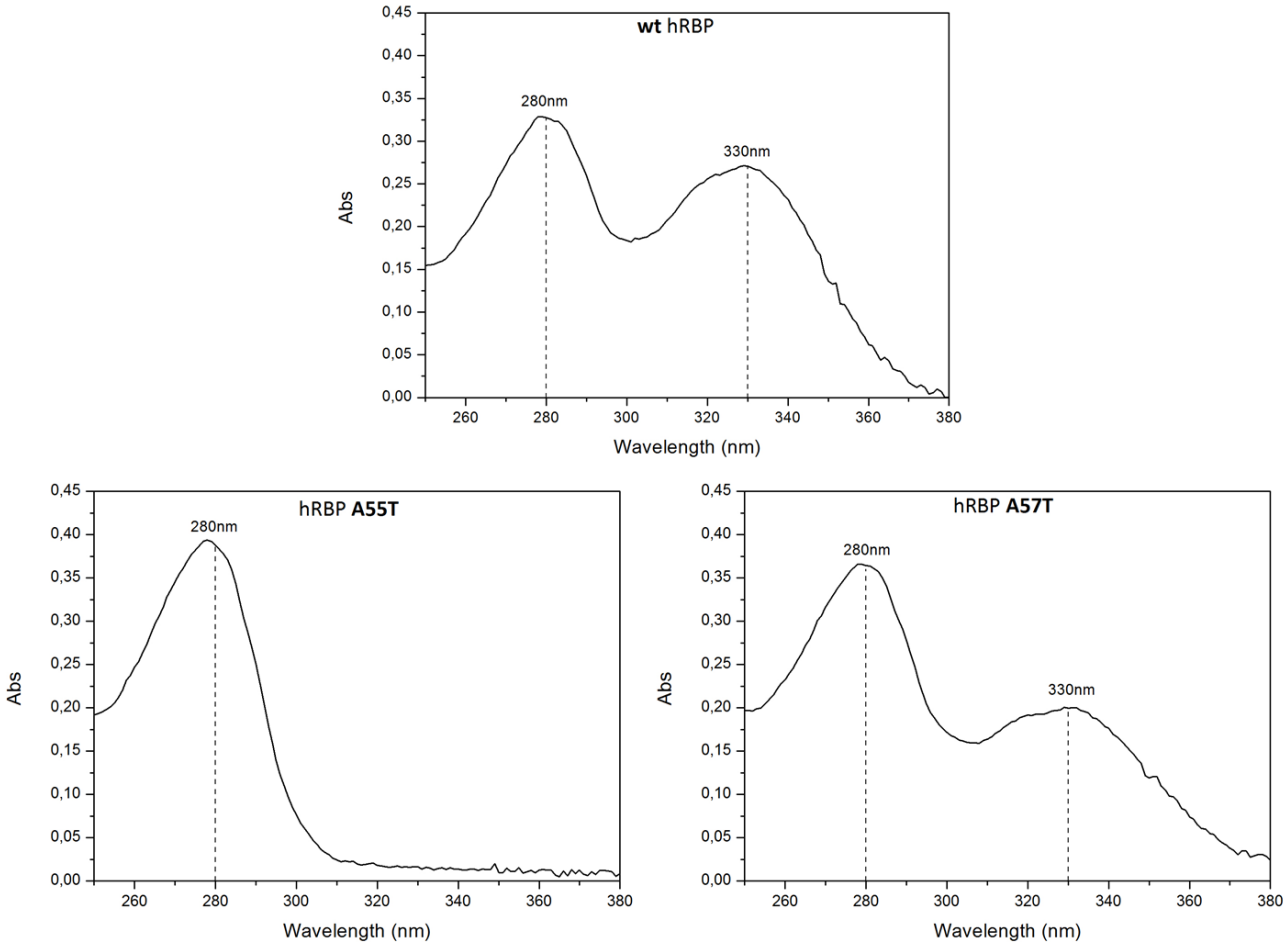

Figure 33. Absorption spectra of purified wt, A55T and A57T hRBP

To understand if it would be possible to improve 280:330 nm ratio and in particular to understand if the refolded hRBP A55T is able to bind the physiological ligand, retinol was added to the different RBP forms. Addition of retinol to hRBP A55T led to the appearance of an absorbance peak at 330nm, showing that the mutant form is able to bind retinol, despite the previous result. Regarding hRBP A57T it was found an increase of the ratio (280:330) up to 0.7, equal to that of hRBP A55T (**Figure 34**). Therefore, it can be concluded that the refolding method is able to generate correctly folded RBP mutant forms which show the ability to bind retinol, although with a reduced affinity as compared to wt hRBP. The retinol could be bound and released during the refolding process. The observed lower affinity of mutant RBP for retinol is in accordance with data obtained in the work of Chou et al. (2015).

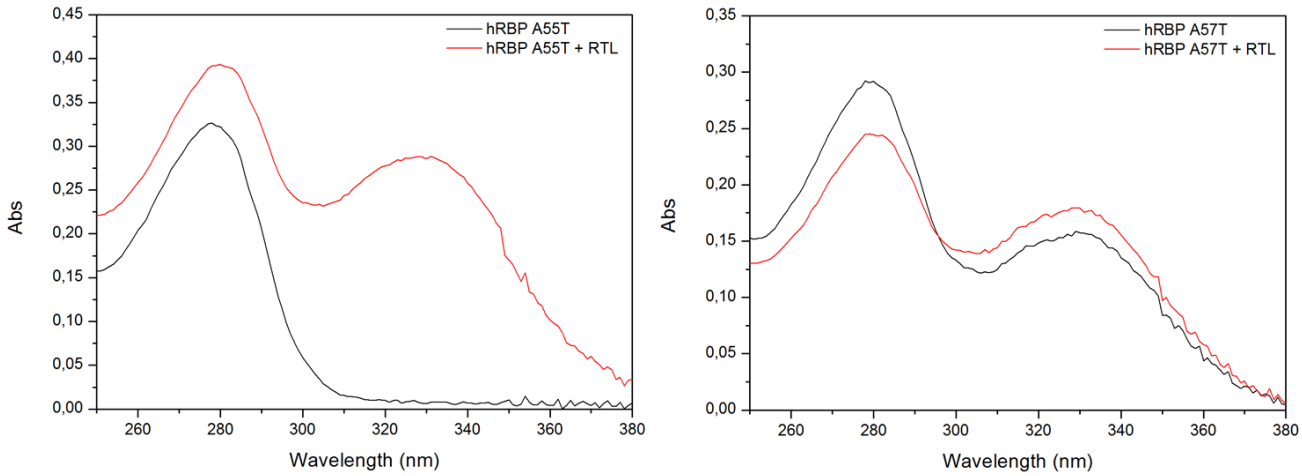

Figure 34. Absorption spectra of hRBP A55T and A57T before and after retinol (RTL) addition

5.3 TTR-RBP affinity chromatography

None of the three hRBP forms show the ideal aforementioned absorption spectrum, even the retinol addition to wt hRBP lead to the increase of the initial absorbance ratio (280:330) above 0.8. Therefore, it was hypothesized that hRBP variants consist of a mixed population of protein molecules, composed by correctly folded and not correctly folded proteins, able to bind or unable to bind retinol, respectively. To achieve a separation between these forms, an affinity chromatography procedure was used, taking advantage of the highly specific TTR-RBP interaction. A matrix consisting of NHS pre-activated Sepharose resin was functionalized with TTR, and the ability of the TTR-coupled matrix to discriminate between apo, holo and uncorrectly folded RBP was evaluated. A partially saturated wt holo-RBP was applied to the column and the elution of

protein was obtained by decreasing the ionic strength of the mobile phase. At low ionic strength, at which the TTR-RBP complex is known to be weak a large absorbance peak was obtained, in which holo-RBP eluted with an absorption ratio (280:330) equal to 1. The chromatography was also performed for the hRBP mutants A55T and A57T and the same elution profile was observed, allowing us to obtain correctly folded holo-RBPs with an absorption ratio (280:330) equal or proximal to 1 (**Figure 35**).

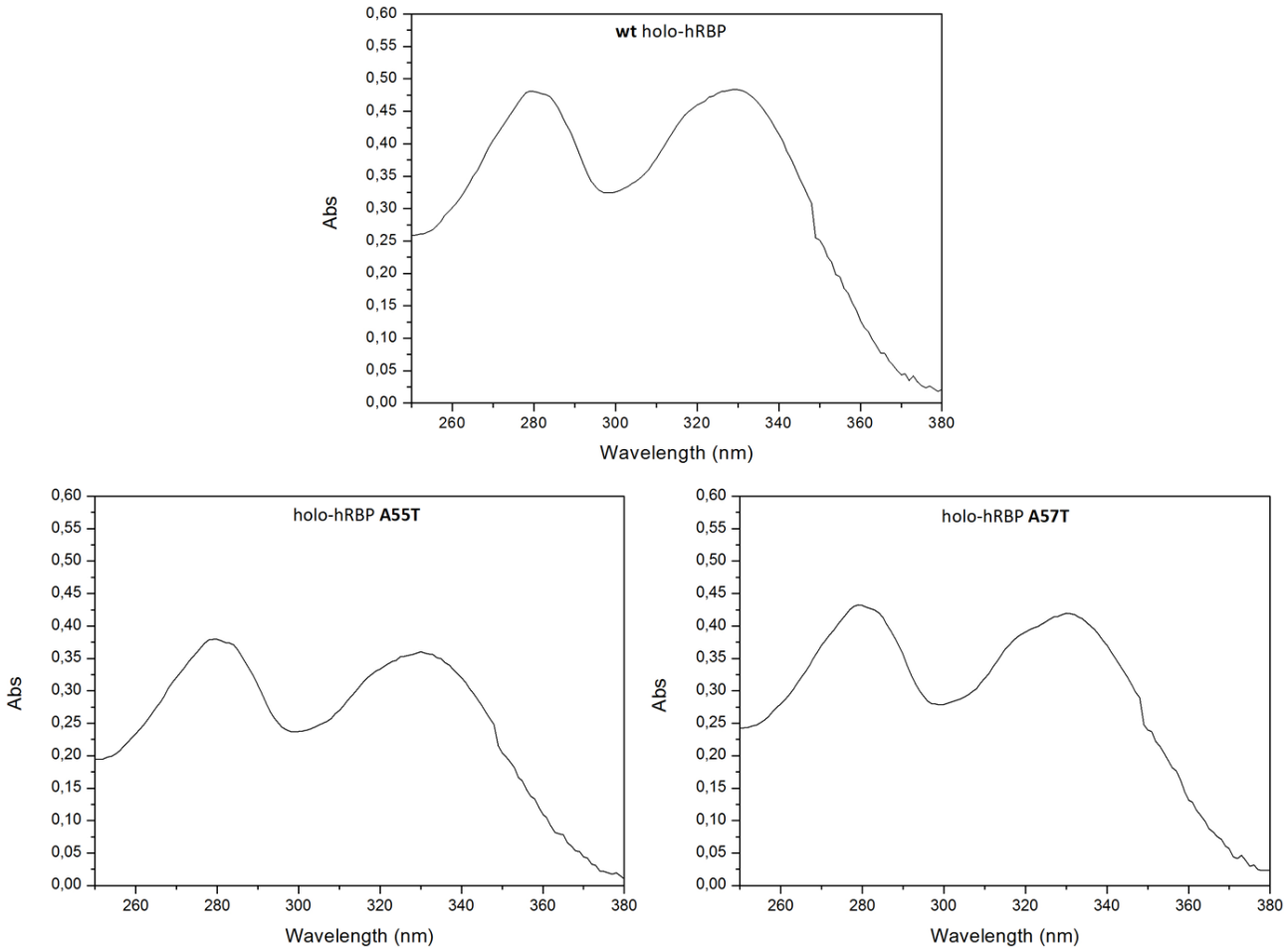

Figure 35. Absorption spectra of the holo forms of wt, A55T and A57T hRBP after affinity chromatography

5.4 RBP-Retinol complex stability

In order to verify the stability of the RBP-retinol complex for the three refolded proteins, aliquots of holo-RBP mutant forms were subjected to spectrophotometric analysis, recording their absorption spectra over time (**Figure 36**). The results do not show a worsening of the absorbance ratio 280:330 nm, indicating a high stability of the complex up to 16 hour incubation at room temperature.

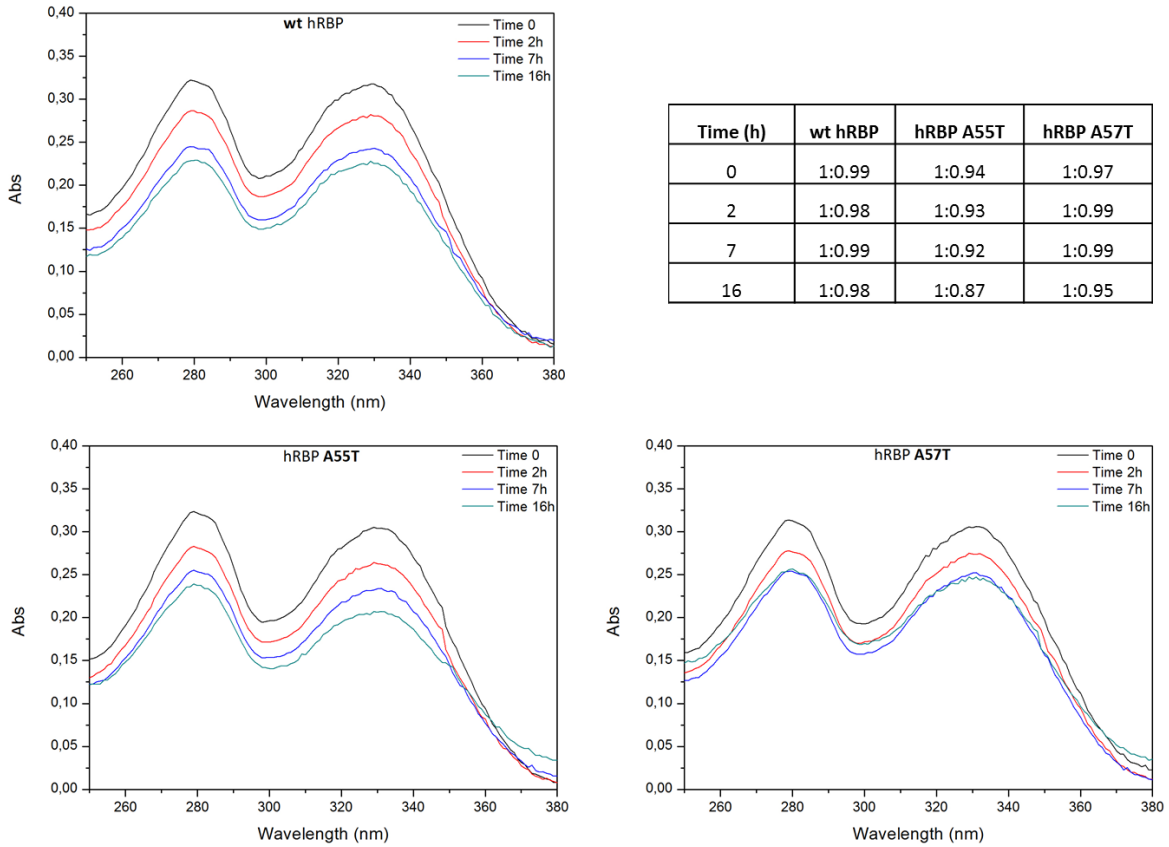

Time (h)	wt hRBP	hRBP A55T	hRBP A57T
0	1:0.99	1:0.94	1:0.97
2	1:0.98	1:0.93	1:0.99
7	1:0.99	1:0.92	1:0.99
16	1:0.98	1:0.87	1:0.95

Figure 36. Absorption spectra of the holo forms of wt hRBP and hRBP A55T and A57T over time. The values of the 280:330 ratio for each spectrum are shown in the table

The retinol release was subsequently monitored by fluorescent measurement after incubation in the presence or in the absence of 8M urea, monitoring the decrease of the fluorescence emission of retinol over time (**Figure 37**). The retinol release from the wt holo-RBP and mutant forms was similar in the absence of urea, while in the presence of 8M urea the kinetics of retinol release were significantly faster for mutant forms, especially for the A55T mutant, as compared to wt hRBP.

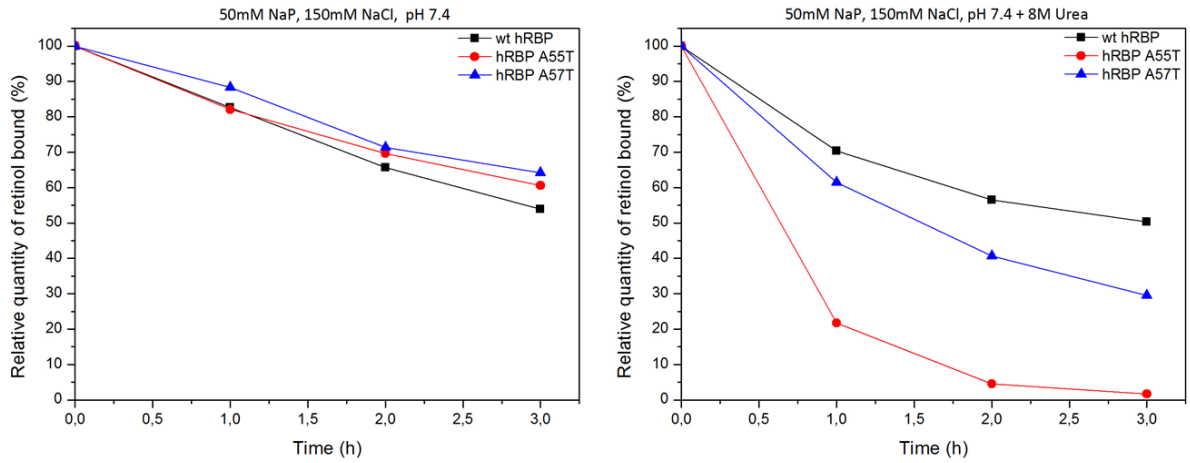

Figure 37. Retinol release for wt , A55T and A57T hRBP in the presence and in the absence of urea

5.5 TTR-RBP interaction

The affinity of holo-RBP mutant forms for TTR was determined by means of fluorescence anisotropy measurements. Holo-hRBPs were titrated with TTR and the corresponding Kd values determined. Representative titrations and the very similar corresponding Kd values are shown in **Figure 38**. Our data further indicate the maintenance of functional properties of RBP mutant forms as compared to the wt protein.

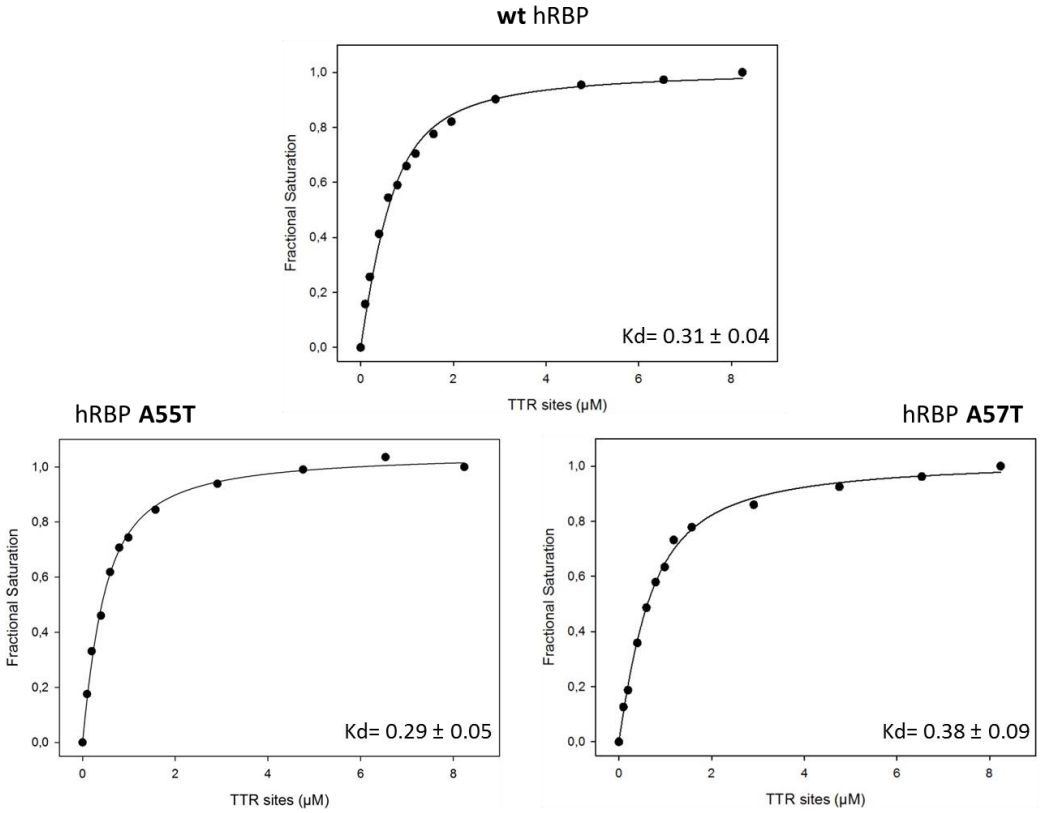

Figure 38. Anisotropy titrations for holo-hRBP variants

5.7 RBP A57T structure

Both holo-hRBP A55T and A57T could be crystallized in conditions suitable for the crystallization of wt holo-RBP. However, single crystal of mutated RBP could be obtained and examined by X-ray analysis (performed by Professor Giuseppe Zanotti from University of Padua) only for the holo-RBP A57T mutant forms (1.6Å resolution). The superposition of holo-hRBP A57T and wt holo-hRBP structures (**Figure 39**) has revealed nearly identical structure with a rmsd of the Cα atoms of 0,4995. Also, the retinol bound inside the cavities of the two proteins in the cavity does not show significant differences. In conclusion the crystal structure of the holo-RBP A57T does not provide evidence for structural alterations of the mutated protein relative to wt holo-RBP.

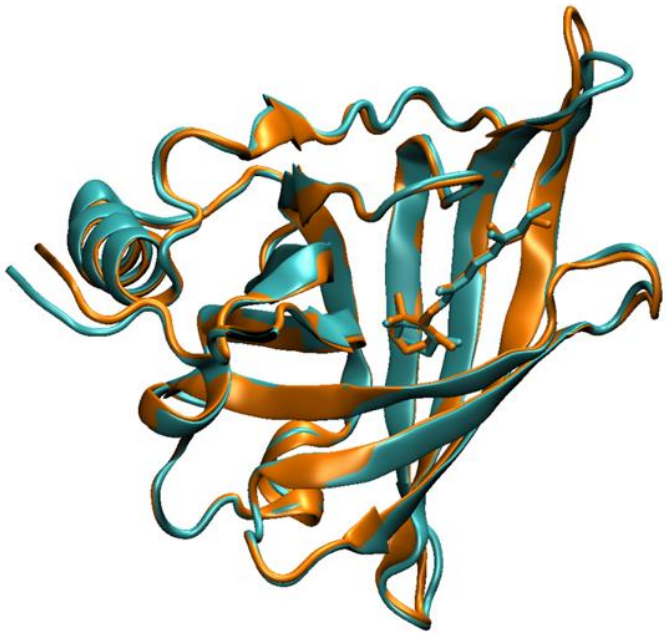

Figure 39. Superprositon of wt holo-hRBP (cyan) (PDB ID: 1RBP) and holo-hRBP A57T (orange). The structure representation was obtained by using Visual Molecular Dynamics (VMD) (Humphrey, Dalke, and Schulten 1996).

5.8 Discussion

The expression of recombinant wt and mutated hRBPs in the *E.coli* host, followed by unfolding and subsequent refolding in the presence of retinol and TTR affinity chromatography, has allowed us to obtain holo-hRBP A55T and A57T, fully saturated by retinol. Moreover the two RBP mutant forms interact with TTR with an affinity similar to that typically of wt holo-RBP. In addition, the high resolution crystal structure of the A57T mutant form is virtually identically with that of the wt holo-RBP. Despite the latter functional and structural evidence, a significant higher instability in denaturing conditions has been revealed for the holo-RBP mutant forms, especially in the case of the A55T mutant. A destabilization of the RBP mutant forms, which was also suggested by Chou et al. (2015), may lead to an impairment of the functional properties of RBP, eventually responsible for the observed pathological alterations.

BIBLIOGRAPHY

Ackermann, EJ, Guo, S, Booten, S, Alvarado, L, Benson, M, Hughes, S, and Monia, BP.(2012) "Clinical Development of an Antisense Therapy for the Treatment of Transthyretin-Associated Polyneuropathy." *Amyloid* 19(sup1): 43–44.

Ankarcrona, M, Winblad, B, Monteiro, C, Fearns, C, Powers, ET, Johansson, J, Westermark, GT, Presto, J, Ericzon, B-G, and Kelly, JW.(2016) "Current and Future Treatment of Amyloid Diseases." *Journal of internal medicine* 280(2): 177–202.

Bartalena, L, and Robbins, J.(1993a) "Thyroid Hormone Transport Proteins." *Clinics in laboratory medicine* 13(3): 583–98.

Baures, PW, Peterson, SA, and Kelly, JW.(1998) "Discovering Transthyretin Amyloid Fibril Inhibitors by Limited Screening." *Bioorganic & medicinal chemistry* 6(8): 1389–1401.

van Bennekum, AM, Wei, S, Gamble, M V., Vogel, S, Piantedosi, R, Gottesman, M, Episkopou, V, and Blaner, WS.(2001) "Biochemical Basis for Depressed Serum Retinol Levels in Transthyretin-Deficient Mice." *Journal of Biological Chemistry* 276(2): 1107–13.

Benson, MD, and Kincaid, JC.(2007) "The Molecular Biology and Clinical Features of Amyloid Neuropathy." *Muscle & Nerve* 36(4): 411–23.

Benson, MD, Kluve-Beckerman, B, Zeldenrust, SR, Siesky, AM, Bodenmiller, DM, Showalter, AD, and Sloop, KW.(2006) "Targeted Suppression of an Amyloidogenic Transthyretin with Antisense Oligonucleotides." *Muscle & Nerve* 33(5): 609–18.

Benson, MD, Smith, A, R, Hung, G, Kluve-Beckerman, B, Showalter, AD, Sloop, KW, and Monia, BP.(2010) "Suppression of Choroid Plexus Transthyretin Levels by Antisense Oligonucleotide Treatment." *Amyloid : the international journal of experimental and clinical investigation : the official journal of the International Society of Amyloidosis* 17(2): 43–49.

Berk, JL, Suhr, OB, Obici, L, Sekijima, Y, Zeldenrust, SR, Yamashita, T, Heneghan, MA, Gorevic, PD, Litchy, WJ, Wiesman, JF, Nordh, E, Corato, M, Lozza, A, Cortese, A, Robinson-Papp, J, Colton, T, Rybin, D V., Bisbee, AB, Ando, Y, et al.(2013) "Repurposing Diflunisal for Familial Amyloid Polyneuropathy." *JAMA* 310(24): 2658.

Berni, R, Malpeli, G, Folli, C, Murrell, JR, Liepnieks, JJ, and Benson, MD.(1994) "The Ile-84-->Ser Amino Acid Substitution in Transthyretin Interferes with the Interaction with Plasma Retinol-Binding Protein." *The Journal of biological chemistry* 269(38): 23395–98.

Biesalski, HK, Frank, J, Beck, SC, Heinrich, F, Illek, B, Reifen, R, Gollnick, H, Seeliger, MW, Wissinger, B, and Zrenner, E.(1999) "Biochemical but Not Clinical Vitamin A Deficiency Results from Mutations in the Gene for Retinol Binding Protein." *The American journal of clinical nutrition* 69(5): 931–36.

Blake, C, and Serpell, L.(1996) "Synchrotron X-Ray Studies Suggest That the Core of the Transthyretin Amyloid Fibril Is a Continuous β-Sheet Helix." *Structure* 4(8): 989–98.

Blake, CC, Geisow, MJ, Oatley, SJ, Rérat, B, and Rérat, C.(1978) "Structure of Prealbumin: Secondary, Tertiary and Quaternary Interactions Determined by Fourier Refinement at 1.8 A." *Journal of molecular biology* 121(3): 339–56.

Blomhoff, R, and Blomhoff, HK.(2006) “Overview of Retinoid Metabolism and Function.” *Journal of neurobiology* 66(7): 606–30.

Bolognesi, B, Kumita, JR, Barros, TP, Esbjorner, EK, Luheshi, LM, Crowther, DC, Wilson, MR, Dobson, CM, Favrin, G, and Yerbury, JJ.(2010) “ANS Binding Reveals Common Features of Cytotoxic Amyloid Species.” *ACS chemical biology* 5(8): 735–40.

Brandstatter, A, Kiechl, S, Kollerits, B, Hunt, SC, Heid, IM, Coassin, S, Willeit, J, Adams, TD, Illig, T, Hopkins, PN, and Kronenberg, F.(2008) “Sex-Specific Association of the Putative Fructose Transporter SLC2A9 Variants With Uric Acid Levels Is Modified by BMI.” *Diabetes Care* 31(8): 1662–67.

Bulawa, CE, Connelly, S, DeVit, M, Wang, L, Weigel, C, Fleming, JA, Packman, J, Powers, ET, Wiseman, RL, Foss, TR, Wilson, IA, Kelly, JW, and Labaudiniere, R.(2012) “Tafamidis, a Potent and Selective Transthyretin Kinetic Stabilizer That Inhibits the Amyloid Cascade.” *Proceedings of the National Academy of Sciences* 109(24): 9629–34.

Casey, J, Kawaguchi, R, Morrissey, M, Sun, H, McGettigan, P, Nielsen, JE, Conroy, J, Regan, R, Kenny, E, Cormican, P, Morris, DW, Tormey, P, Chróinín, MN, Kennedy, BN, Lynch, S, Green, A, and Ennis, S.(2011) “First Implication of STRA6 Mutations in Isolated Anophthalmia, Microphthalmia, and Coloboma: A New Dimension to the STRA6 Phenotype.” *Human mutation* 32(12): 1417–26.

Cendron, L, Ramazzina, I, Percudani, R, Rasore, C, Zanotti, G, and Berni, R.(2011) “Probing the Evolution of Hydroxyisourate Hydrolase into Transthyretin through Active-Site Redesign.” *Journal of Molecular Biology* 409(4): 504–12.

Chassaing, N, Golzio, C, Odent, S, Lequeux, L, Vigouroux, A, Martinovic-Bouriel, J, Tiziano, FD, Masini, L, Piro, F, Maragliano, G, Delezoide, A-L, Attié-Bitach, T, Manouvrier-Hanu, S, Etchevers, HC, and Calvas, P.(2009) “Phenotypic Spectrum of STRA6 Mutations: From Matthew-Wood Syndrome to Non-Lethal Anophthalmia.” *Human mutation* 30(5): E673-81.

Chen, Y, Clarke, OB, Kim, J, Stowe, S, Kim, Y-K, Assur, Z, Cavalier, M, Godoy-Ruiz, R, von Alpen, DC, Manzini, C, Blaner, WS, Frank, J, Quadro, L, Weber, DJ, Shapiro, L, Hendrickson, WA, and Mancia, F.(2016) “Structure of the STRA6 Receptor for Retinol Uptake.” *Science (New York, N.Y.)* 353(6302).

Chou, CM, Nelson, C, Tarlé, SA, Pribila, JT, Bardakjian, T, Woods, S, Schneider, A, and Glaser, T.(2015) “Biochemical Basis for Dominant Inheritance, Variable Penetrance, and Maternal Effects in RBP4 Congenital Eye Disease.” *Cell* 161(3): 634–46.

Cianci, M, Folli, C, Zonta, F, Florio, P, Berni, R, and Zanotti, G.(2015) “Structural Evidence for Asymmetric Ligand Binding to Transthyretin.” *Acta Crystallographica Section D Biological Crystallography* 71(8): 1582–92.

Coelho, T, Adams, D, Silva, A, Lozeron, P, Hawkins, PN, Mant, T, Perez, J, Chiesa, J, Warrington, S, Tranter, E, Munisamy, M, Falzone, R, Harrop, J, Cehelsky, J, Bettencourt, BR, Geissler, M, Butler, JS, Sehgal, A, Meyers, RE, et al.(2013) “Safety and Efficacy of RNAi Therapy for Transthyretin Amyloidosis.” *New England Journal of Medicine* 369(9): 819–29.

Coelho, T, Maia, LF, Martins da Silva, A, Waddington Cruz, M, Planté-Bordeneuve, V, Lozeron, P, Suhr, OB, Campistol, JM, Conceição, IM, Schmidt, HH-J, Trigo, P, Kelly, JW, Labaudinière, R, Chan, J, Packman, J, Wilson, A, and Grogan, DR.(2012) "Tafamidis for Transthyretin Familial Amyloid Polyneuropathy: A Randomized, Controlled Trial." *Neurology* 79(8): 785–92.

Colon, W, and Kelly, JW.(1992) "Partial Denaturation of Transthyretin Is Sufficient for Amyloid Fibril Formation in Vitro." *Biochemistry* 31(36): 8654–60.

Connelly, S, Choi, S, Johnson, SM, Kelly, JW, and Wilson, IA.(2010) "Structure-Based Design of Kinetic Stabilizers That Ameliorate the Transthyretin Amyloidoses." *Current opinion in structural biology* 20(1): 54–62.

Connors, LH, Lim, A, Prokaeva, T, Roskens, VA, and Costello, CE.(2003) "Tabulation of Human Transthyretin (TTR) Variants, 2003." *Amyloid : the international journal of experimental and clinical investigation : the official journal of the International Society of Amyloidosis* 10(3): 160–84.

Cowan, SW, Newcomer, ME, and Jones, TA.(1990) "Crystallographic Refinement of Human Serum Retinol Binding Protein at 2Å Resolution." *Proteins: Structure, Function, and Genetics* 8(1): 44–61.

Dickson, PW, Aldred, AR, Menting, JG, Marley, PD, Sawyer, WH, and Schreiber, G.(1987) "Thyroxine Transport in Choroid Plexus." *The Journal of biological chemistry* 262(29): 13907–15.

Dobson, CM.(2003) "Protein Folding and Misfolding." *Nature* 426(6968): 884–90.

Dowling, JE, and Wald, G.(1958) "Vitamin A Deficiency and Night Blindness." *Proceedings of the National Academy of Sciences of the United States of America* 44(7): 648–61.

Duester, G.(2009) "Keeping an Eye on Retinoic Acid Signaling during Eye Development." *Chemico-Biological Interactions* 178(1–3): 178–81.

Episkopou, V, Maeda, S, Nishiguchi, S, Shimada, K, Gaitanaris, GA, Gottesman, ME, and Robertson, EJ.(1993) "Disruption of the Transthyretin Gene Results in Mice with Depressed Levels of Plasma Retinol and Thyroid Hormone." *Proceedings of the National Academy of Sciences of the United States of America* 90(6): 2375–79.

Fändrich, M.(2012) "Oligomeric Intermediates in Amyloid Formation: Structure Determination and Mechanisms of Toxicity." *Journal of Molecular Biology* 421(4–5): 427–40.

Ferguson, RN, Edelhoch, H, Saroff, HA, Robbins, J, and Cahnmann, HJ.(1975) "Negative Cooperativity in the Binding of Thyroxine to Human Serum Prealbumin. Preparation of Tritium-Labeled 8-Anilino-1-Naphthalenesulfonic Acid." *Biochemistry* 14(2): 282–89.

Fex, G, Albertsson, PA, and Hansson, B.(1979) "Interaction between Prealbumin and Retinol-Binding Protein Studied by Affinity Chromatography, Gel Filtration and Two-Phase Partition." *European journal of biochemistry* 99(2): 353–60.

Florio, P, Folli, C, Cianci, M, Del Rio, D, Zanotti, G, and Berni, R.(2015) "Transthyretin Binding Heterogeneity and Anti-Amyloidogenic Activity of Natural Polyphenols and Their Metabolites." *Journal of Biological Chemistry* 290(50): 29769–80.

Folli, C, Viglione, S, Busconi, M, and Berni, R.(2005a) “Biochemical Basis for Retinol Deficiency Induced by the I41N and G75D Mutations in Human Plasma Retinol-Binding Protein.” *Biochemical and Biophysical Research Communications* 336(4): 1017–22.

French, JB, and Ealick, SE.(2011) “Structural and Kinetic Insights into the Mechanism of 5-Hydroxyisourate Hydrolase from Klebsiella Pneumoniae.” *Acta crystallographica. Section D, Biological crystallography* 67(Pt 8): 671–77.

Gasparini, L, Rusconi, L, Xu, H, del Soldato, P, and Ongini, E.(2004) “Modulation of Beta-Amyloid Metabolism by Non-Steroidal Anti-Inflammatory Drugs in Neuronal Cell Cultures.” *Journal of neurochemistry* 88(2): 337–48.

Gliozzi, M, Malara, N, Muscoli, S, and Mollace, V.(2016) “The Treatment of Hyperuricemia.” *International Journal of Cardiology* 213: 23–27.

Goodman, DS, and Raz, A.(1972) “Extraction and Recombination Studies of the Interaction of Retinol with Human Plasma Retinol-Binding Protein.” *Journal of lipid research* 13(3): 338–47.

Graessler, J, Graessler, A, Unger, S, Kopprasch, S, Tausche, A-K, Kuhlisch, E, and Schroeder, H-E.(2006) “Association of the Human Urate Transporter 1 with Reduced Renal Uric Acid Excretion and Hyperuricemia in a German Caucasian Population.” *Arthritis & Rheumatism* 54(1): 292–300.

van Groen, T, and Kadish, I.(2005) “Transgenic AD Model Mice, Effects of Potential Anti-AD Treatments on Inflammation and Pathology.” *Brain Research Reviews* 48(2): 370–78.

Haass, C, and Selkoe, DJ.(2007) “Soluble Protein Oligomers in Neurodegeneration: Lessons from the Alzheimer’s Amyloid β-Peptide.” *Nature Reviews Molecular Cell Biology* 8(2): 101–12.

Hammarström, P, Jiang, X, Hurshman, AR, Powers, ET, and Kelly, JW.(2002) “Sequence-Dependent Denaturation Energetics: A Major Determinant in Amyloid Disease Diversity.” *Proceedings of the National Academy of Sciences of the United States of America* 99 Suppl 4: 16427–32.

Hammarström, P, Wiseman, RL, Powers, ET, and Kelly, JW.(2003) “Prevention of Transthyretin Amyloid Disease by Changing Protein Misfolding Energetics.” *Science (New York, N.Y.)* 299(5607): 713–16.

Haupt, M, Blakeley, MP, Fisher, SJ, Mason, SA, Cooper, JB, Mitchell, EP, and Forsyth, VT.(2014) “Binding Site Asymmetry in Human Transthyretin: Insights from a Joint Neutron and X-Ray Crystallographic Analysis Using Perdeuterated Protein.” *IUCrJ* 1(6): 429–38.

Hennebry, SC, Law, RHP, Richardson, SJ, Buckle, AM, and Whisstock, JC.(2006) “The Crystal Structure of the Transthyretin-like Protein from Salmonella Dublin, a Prokaryote 5-Hydroxyisourate Hydrolase.” *Journal of Molecular Biology* 359(5): 1389–99.

Hörnberg, a, Eneqvist, T, Olofsson, A, Lundgren, E, and Sauer-Eriksson, a E.(2000) “A Comparative Analysis of 23 Structures of the Amyloidogenic Protein Transthyretin.” *Journal of molecular biology* 302(3): 649–69.

Hou, X, Parkington, HC, Coleman, HA, Mechler, A, Martin, LL, Aguilar, M-I, and Small, DH.(2007) “Transthyretin Oligomers Induce Calcium Influx via Voltage-Gated Calcium Channels.” *Journal of Neurochemistry* 100(2): 446–57.

Humphrey, W, Dalke, A, and Schulten, K.(1996) “VMD: Visual Molecular Dynamics.” *Journal of molecular graphics* 14(1): 33–38, 27–28.

Hurshman, AR, White, JT, Powers, ET, and Kelly, JW.(2004) “Transthyretin Aggregation under Partially Denaturing Conditions Is a Downhill Polymerization.” *Biochemistry* 43(23): 7365–81.

Jorga, KM, Sedek, G, Fotteler, B, Zürcher, G, Nielsen, T, and Aitken, JW.(1997) “Optimizing Levodopa Pharmacokinetics with Multiple Tolcapone Doses in the Elderly.” *Clinical pharmacology and therapeutics* 62(3): 300–310.

Jung, D-K, Lee, Y, Park, SG, Park, BC, Kim, G-H, and Rhee, S.(2006) “Structural and Functional Analysis of PucM, a Hydrolase in the Ureide Pathway and a Member of the Transthyretin-Related Protein Family.” *Proceedings of the National Academy of Sciences* 103(26): 9790–95.

Kawaguchi, R, Yu, J, Honda, J, Hu, J, Whitelegge, J, Ping, P, Wiita, P, Bok, D, and Sun, H.(2007) “A Membrane Receptor for Retinol Binding Protein Mediates Cellular Uptake of Vitamin A.” *Science* 315(5813): 820–25.

Kelly, JW.(1996) “Alternative Conformations of Amyloidogenic Proteins Govern Their Behavior.” *Current opinion in structural biology* 6(1): 11–17.

Klabunde, T, Petrassi, HM, Oza, VB, Raman, P, Kelly, JW, and Sacchettini, JC.(2000) “Rational Design of Potent Human Transthyretin Amyloid Disease Inhibitors.” *Nature structural biology* 7(4): 312–21.

Lai, Z, Colón, W, and Kelly, JW.(1996) “The Acid-Mediated Denaturation Pathway of Transthyretin Yields a Conformational Intermediate That Can Self-Assemble into Amyloid.” *Biochemistry* 35(20): 6470–82.

Lesch, M, and Nyhan, WL.(1964) “A Familial Disorder of Uric Acid Metabolism and Central Nervous System Function.” *The American journal of medicine* 36: 561–70.

Lim, GP, Yang, F, Chu, T, Chen, P, Beech, W, Teter, B, Tran, T, Ubeda, O, Ashe, KH, Frautschy, SA, and Cole, GM.(2000) “Ibuprofen Suppresses Plaque Pathology and Inflammation in a Mouse Model for Alzheimer’s Disease.” *The Journal of neuroscience : the official journal of the Society for Neuroscience* 20(15): 5709–14.

Malpeli, G, Folli, C, and Berni, R.(1996) “Retinoid Binding to Retinol-Binding Protein and the Interference with the Interaction with Transthyretin.” *Biochimica et biophysica acta* 1294(1): 48–54.

McCammon, MG, Scott, DJ, Keetch, CA, Greene, LH, Purkey, HE, Petrassi, HM, Kelly, JW, and Robinson, C V.(2002) “Screening Transthyretin Amyloid Fibril Inhibitors: Characterization of Novel Multiprotein, Multiligand Complexes by Mass Spectrometry.” *Structure (London, England : 1993)* 10(6): 851–63.

Miller, SR, Sekijima, Y, and Kelly, JW.(2004) “Native State Stabilization by NSAIDs Inhibits Transthyretin Amyloidogenesis from the Most Common Familial Disease Variants.” *Laboratory Investigation* 84(5): 545–52.

Miroy, GJ, Lai, Z, Lashuel, HA, Peterson, SA, Strang, C, and Kelly, JW.(1996) "Inhibiting Transthyretin Amyloid Fibril Formation via Protein Stabilization." *Proceedings of the National Academy of Sciences of the United States of America* 93(26): 15051–56.

Monaco, HL, Rizzi, M, and Coda, A.(1995a) "Structure of a Complex of Two Plasma Proteins: Transthyretin and Retinol-Binding Protein." *Science* 268(5213): 1039–41.

Mu, Y, Jin, S, Shen, J, Sugano, A, Takaoka, Y, Qiang, L, Imbimbo, BP, Yamamura, K, and Li, Z.(2015) "CHF5074 (CSP-1103) Stabilizes Human Transthyretin in Mice Humanized at the Transthyretin and Retinol-Binding Protein Loci." *FEBS Letters* 589(7): 849–56.

Muzioł, T, Cody, V, and Wojtczak, A.(2001) "Comparison of Binding Interactions of Dibromoflavonoids with Transthyretin." *Acta biochimica Polonica* 48(4): 885–92.

Naylor, HM, and Newcomer, ME.(1999) "The Structure of Human Retinol-Binding Protein (RBP) with Its Carrier Protein Transthyretin Reveals an Interaction with the Carboxy Terminus of RBP." *Biochemistry* 38(9): 2647–53.

Nicholas, and Nicholas, H.(1997) "GeneDoc: A Tool for Editing and Annotating Multiple Sequence Alignments." *Distributed by the author. http://www.psc.edu/biomed/genedoc*.

Nilsson, L, Larsson, A, Begum, A, Iakovleva, I, Carlsson, M, Brännström, K, Sauer-Eriksson, AE, and Olofsson, A.(2016) "Modifications of the 7-Hydroxyl Group of the Transthyretin Ligand Luteolin Provide Mechanistic Insights into Its Binding Properties and High Plasma Specificity." *PLoS ONE* 11(4): 1–19.

Nuernberg, B, Koehler, G, and Brune, K.(1991) "Pharmacokinetics of Diflunisal in Patients." *Clinical Pharmacokinetics* 20(1): 81–89.

Oda, M, Satta, Y, Takenaka, O, and Takahata, N.(2002) "Loss of Urate Oxidase Activity in Hominoids and Its Evolutionary Implications." *Molecular biology and evolution* 19(5): 640–53.

Peretto, I, Radaelli, S, Parini, C, Zandi, M, Raveglia, LF, Dondio, G, Fontanella, L, Misiano, P, Bigogno, C, Rizzi, A, Riccardi, B, Biscaioli, M, Marchetti, S, Puccini, P, Catinella, S, Rondelli, I, Cenacchi, V, Bolzoni, PT, Caruso, P, et al.(2005) "Synthesis and Biological Activity of Flurbiprofen Analogues as Selective Inhibitors of Beta-amyloid(1)(-)(42) Secretion." *Journal of medicinal chemistry* 48(18): 5705–20.

Pullakhandam, R, Srinivas, PNBS, Nair, MK, and Reddy, GB.(2009) "Binding and Stabilization of Transthyretin by Curcumin." *Archives of Biochemistry and Biophysics* 485(2): 115–19.

Radović, B, Mentrup, B, and Köhrle, J.(2006) "Genistein and Other Soya Isoflavones Are Potent Ligands for Transthyretin in Serum and Cerebrospinal Fluid." *The British journal of nutrition* 95(6): 1171–76.

Ramazzina, I, Folli, C, Secchi, A, Berni, R, and Percudani, R.(2006) "Completing the Uric Acid Degradation Pathway through Phylogenetic Comparison of Whole Genomes." *Nature Chemical Biology* 2(3): 144–48.

Razavi, H, Palaninathan, SK, Powers, ET, Wiseman, RL, Purkey, HE, Mohamedmohaideen, NN, Deechongkit, S, Chiang, KP, Dendle, MTA, Sacchettini, JC, and Kelly, JW.(2003) "Benzoxazoles as Transthyretin Amyloid Fibril Inhibitors: Synthesis, Evaluation, and Mechanism of Action." *Angewandte Chemie International Edition* 42(24): 2758–61.

Redondo, C, Vouropoulou, M, Evans, J, and Findlay, JBC.(2007) "Identification of the Retinol-Binding Protein (RBP) Interaction Site and Functional State of RBPs for the Membrane Receptor." *The FASEB Journal* 22(4): 1043–54.

Reixach, N, Deechongkit, S, Jiang, X, Kelly, JW, and Buxbaum, JN.(2004) "Tissue Damage in the Amyloidoses: Transthyretin Monomers and Nonnative Oligomers Are the Major Cytotoxic Species in Tissue Culture." *Proceedings of the National Academy of Sciences* 101(9): 2817–22.

Richardson, SJ.(2005) "Developmentally Regulated Thyroid Hormone Distributor Proteins in Marsupials, a Reptile, and Fish." *AJP: Regulatory, Integrative and Comparative Physiology* 288(5): R1264–72.

Richardson, SJ, Wijayagunaratne, RC, D'Souza, DG, Darras, VM, and Van Herck, SLJ.(2015) "Transport of Thyroid Hormones via the Choroid Plexus into the Brain: The Roles of Transthyretin and Thyroid Hormone Transmembrane Transporters." *Frontiers in Neuroscience* 9(MAR): 1–8.

Robinson, LZ, and Reixach, N.(2014) "Quantification of Quaternary Structure Stability in Aggregation-Prone Proteins under Physiological Conditions: The Transthyretin Case." *Biochemistry* 53(41): 6496–6510.

Sant'Anna, R, Gallego, P, Robinson, LZ, Pereira-Henriques, A, Ferreira, N, Pinheiro, F, Esperante, S, Pallares, I, Huertas, O, Rosário Almeida, M, Reixach, N, Insa, R, Velazquez-Campoy, A, Reverter, D, Reig, N, and Ventura, S.(2016) "Repositioning Tolcapone as a Potent Inhibitor of Transthyretin Amyloidogenesis and Associated Cellular Toxicity." *Nature Communications* 7: 10787.

Santos, XC, Anjos, EI, and Augusto, O.(1999) "Uric Acid Oxidation by Peroxynitrite : Multiple Reactions , Free Radical Formation , and Amplification of Lipid Oxidation." 372(2): 285–94.

Schreiber, G, Aldred, AR, Jaworowski, A, Nilsson, C, Achen, MG, and Segal, MB.(1990) "Thyroxine Transport from Blood to Brain via Transthyretin Synthesis in Choroid Plexus." *The American journal of physiology* 258(2 Pt 2): R338-45.

See, AW-M, and Clagett-Dame, M.(2009) "The Temporal Requirement for Vitamin A in the Developing Eye: Mechanism of Action in Optic Fissure Closure and New Roles for the Vitamin in Regulating Cell Proliferation and Adhesion in the Embryonic Retina." *Developmental Biology* 325(1): 94–105.

Sekijima, Y.(2015) "Transthyretin (ATTR) Amyloidosis: Clinical Spectrum, Molecular Pathogenesis and Disease-Modifying Treatments." *Journal of Neurology, Neurosurgery & Psychiatry* 86(9): 1036–43.

Sekijima, Y, Dendle, MA, and Kelly, JW.(2006) "Orally Administered Diflunisal Stabilizes Transthyretin against Dissociation Required for Amyloidogenesis." *Amyloid* 13(4): 236–49.

Sekijima, Y, Wiseman, RL, Matteson, J, Hammarström, P, Miller, SR, Sawkar, AR, Balch, WE, and Kelly, JW.(2005) “The Biological and Chemical Basis for Tissue-Selective Amyloid Disease.” *Cell* 121(1): 73–85.

Sekijima, Y, Yoshida, K, Tokuda, T, and Ikeda, S.(2012) GeneReviews(®) *Familial Transthyretin Amyloidosis*. University of Washington, Seattle.

Serpell, LC, Sunde, M, and Blake, CC.(1997) “The Molecular Basis of Amyloidosis.” *Cellular and molecular life sciences* 53(11–12): 871–87.

Sipe, JD, Benson, MD, Buxbaum, JN, Ikeda, S, Merlini, G, Saraiva, MJM, and Westermark, P.(2014) “Nomenclature 2014: Amyloid Fibril Proteins and Clinical Classification of the Amyloidosis.” *Amyloid : the international journal of experimental and clinical investigation : the official journal of the International Society of Amyloidosis* 21(4): 221–24.

Sporn, MB, Dunlop, NM, Newton, DL, and Smith, JM.(1976) “Prevention of Chemical Carcinogenesis by Vitamin A and Its Synthetic Analogs (Retinoids).” *Federation proceedings* 35(6): 1332–38.

Sporn, MB, and Roberts, AB.(1985) “What Is a Retinoid?” *Ciba Foundation symposium* 113: 1–5.

Tamura, K, Dudley, J, Nei, M, and Kumar, S.(2007) “MEGA4: Molecular Evolutionary Genetics Analysis (MEGA) Software Version 4.0.” *Molecular Biology and Evolution* 24(8): 1596–99.

Weggen, S, Eriksen, JL, Das, P, Sagi, SA, Wang, R, Pietrzik, CU, Findlay, KA, Smith, TE, Murphy, MP, Bulter, T, Kang, DE, Marquez-Sterling, N, Golde, TE, and Koo, EH.(2001) “A Subset of NSAIDs Lower Amyloidogenic Aβ42 Independently of Cyclooxygenase Activity.” *Nature* 414(6860): 212–16.

Westermark, GT, Fändrich, M, and Westermark, P.(2015) “AA Amyloidosis: Pathogenesis and Targeted Therapy.” *Annual Review of Pathology: Mechanisms of Disease* 10(1): 321–44.

Wilson, JG, Roth, CB, and Warkany, J.(1953) “An Analysis of the Syndrome of Malformations Induced by Maternal Vitamin a Deficiency. Effects of Restoration of Vitamin a at Various Times during Gestation.” *American Journal of Anatomy* 92(2): 189–217.

Wojtczak, A, Cody, V, Luft, JR, and Pangborn, W.(1996) “Structures of Human Transthyretin Complexed with Thyroxine at 2.0 Å Resolution and 3’,5’-Dinitro- N-Acetyl- L -Thyronine at 2.2 Å Resolution.” *Acta Crystallographica Section D Biological Crystallography* 52(4): 758–65.

Xie, Y, Lashuel, HA, Miroy, GJ, Dikler, S, and Kelly, JW.(1998) “Recombinant Human Retinol-Binding Protein Refolding, Native Disulfide Formation, and Characterization.” *Protein expression and purification* 14(1): 31–37.

Zanotti, G, and Berni, R.(2004) “Plasma Retinol-Binding Protein: Structure and Interactions with Retinol, Retinoids, and Transthyretin.” *Vitamins and hormones* 69: 271–95.

Zanotti, G, Cendron, L, Folli, C, Florio, P, Imbimbo, B Pietro, and Berni, R.(2013) “Structural Evidence for Native State Stabilization of a Conformationally Labile Amyloidogenic Transthyretin Variant by Fibrillogenesis Inhibitors.” *FEBS Letters* 587(15): 2325–31.

Zanotti, G, Cendron, L, Ramazzina, I, Folli, C, Percudani, R, and Berni, R.(2006) “Structure of Zebra Fish HIUase: Insights into Evolution of an Enzyme to a Hormone Transporter.” *Journal of Molecular Biology* 363(1): 1–9.

Zanotti, G, Folli, C, Cendron, L, Alfieri, B, Nishida, SK, Gliubich, F, Pasquato, N, Negro, A, and Berni, R.(2008) “Structural and Mutational Analyses of Protein-Protein Interactions between Transthyretin and Retinol-Binding Protein.” *FEBS Journal* 275(23): 5841–54.

Zanotti, G, Ottonello, S, Berni, R, and Monaco, HL.(1993) “Crystal Structure of the Trigonal Form of Human Plasma Retinol-Binding Protein at 2·5 Å Resolution.” *Journal of Molecular Biology* 230(2): 613–24.

Zhao, L, Buxbaum, JN, and Reixach, N.(2013) “Age-Related Oxidative Modifications of Transthyretin Modulate Its Amyloidogenicity.” *Biochemistry* 52(11): 1913–26.